

abnormal immune responses and pronounced synovial hyperplasia. Synovial macrophages are capable of differentiating into osteoclasts; the osteoclasts generated within the synovial membrane are probably involved in bone destruction *in vivo* [16]. Multinucleate cells scoring positive for tartrate-resistant acid phosphatase (TRAP) were also induced from CD14-positive cells in the synovial fluid from patients with RA [17]. TRAP-positive multinucleate cells are present in the bone erosion area of patients with RA [18] and also in the bone erosion area of a mouse arthritis model [19,20]. Although the precise mechanism of joint destruction has not been elucidated, osteoclasts seem to have a pivotal role in the joints of patients with RA.

Specific DNA sequences have been used successfully as decoys for binding specific transcription factors, rendering the transcription factors incapable of subsequent binding to the promoter region of target genes [21,22]. This approach has been shown to be effective in modulating gene expression *in vitro* and *in vivo*. The applications of the decoy oligodeoxynucleotides (ODN) strategy against NF- κ B have been reported in several studies [23-26]. However, one of the major limitations of the decoy ODN approach is the rapid degradation of phosphodiester ODN by intracellular nucleases. Previously, circular dumbbell double-stranded decoy ODN (we call these ribbon-type decoy ODN) were developed to resolve these issues [27,28]. According to the previous reports, ribbon-type decoy ODN tend to bind more specifically to the transcription factors and have stronger resistance to exonuclease [29,30]. In this study, we tried to use ribbon-type NF- κ B decoy ODN for inhibiting the expression of NF- κ B, leading to the inhibition of osteoclast induction and activity.

Materials and methods

Materials

Ribbon-type decoy ODN and phosphorothionated double-stranded decoy ODN were purchased from Gene Design (Osaka, Japan). Mouse RANKL and mouse M-CSF were purchased from Wako (Tokyo, Japan). Lewis rats were purchased from Clea Japan (Osaka, Japan). Bovine type II collagen was purchased from Cosmo Bio (Tokyo, Japan) and Freund's incomplete adjuvant from Sigma (Munich, Germany).

Construction of ribbon-type decoy ODN and phosphorothionated double-stranded decoy ODN

The sequences of ribbon-type decoy ODN and phosphorothionated double-stranded decoy ODN are as follows (consensus sequences are shown in bold): ribbon-type NF- κ B decoy ODN (RNODN), 5'-TCAAGGAAAACCTTGAAG-**GGATTTCCCTCCAAAAGGAGGGAAATCCCT**-3' ; ribbon-type scrambled decoy ODN (RSODN), 5'-TAGCCAAAAGGCTAAGTCAGGTACGGCAAAAATT-GCCGTACCTGACT-3' ; phosphorothionated double-stranded NF- κ B decoy ODN (PNODN), 5'-CCTTGAAG-**GGATTTCCCTCC**-3' and 3'-GGAAC**TTCCCTAAAG**-

GGAGG-5' ; and phosphorothionate double-stranded scrambled decoy ODN (PSODN) 5'-TTGCCGTACCTGACT-TAGCC-3' and 3'-AACGGCATGGACTGAATCGG-5' (Figure 1). Decoy ODN containing the NF- κ B consensus sequence has been shown to bind the NF- κ B transcription factor [24]. PNODN and PSODN were annealed for 2 hours with a steady temperature decrease from 70°C to 25°C. One unit of T4 DNA ligase was added to the mixture, followed by incubation for 24 hours at 22°C to generate a covalently ligated RNODN.

Resistance to exonuclease

To check resistance for exonuclease, electrophoresis of RNODN and PNODN was performed. In brief, 3 μ g of RNODN or PNODN was incubated with exonuclease III at 37°C for 2 hours and then at 65°C for 5 minutes. The solution containing ODN was resolved by electrophoresis on a 19% acrylamide gel.

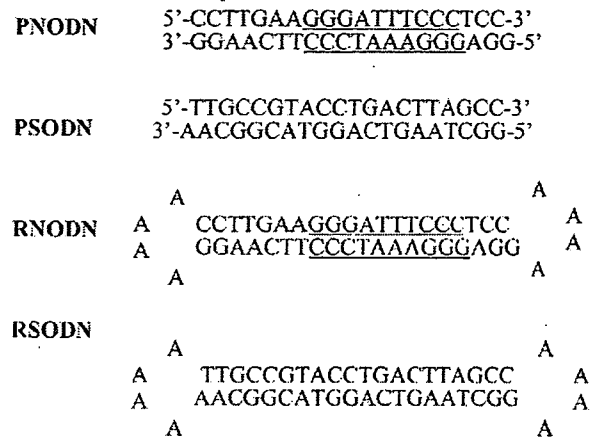
Estimation of binding activity

The binding activity of RNODN was examined by using Mercury Transfactor Kits for NF- κ B p65 (BD Bioscience, Clontech, Palo Alto, CA, USA) as oligonucleotide competition assays. Kits contain a 96-well format in which wells are coated with an oligonucleotide containing the NF- κ B p65 consensus binding sequence. The quantity of nuclear extract binding to the oligonucleotide of the wells is correlated with an increase in signal. An increase in the amount of competitor oligonucleotide corresponds to a decrease in signal because transcription factor binding decreases as the competitor keeps it away from the oligonucleotide-coated surface of the *trans*-Factor well. We estimated the binding activity of oligonucleotides by incubating the same amounts of nuclear protein and various oligonucleotides. An aliquot (30 μ g) of TNF- α -stimulated HeLa nuclear extract (Active Motif, Carlsbad, CA, USA) was incubated with decoy ODN (15, 30, and 45 nM) in *trans*-Factor wells for 60 minutes at room temperature. Wells were incubated with primary and secondary antibodies, and the absorbance of the plate was measured with a microplate reader (Model 680; Bio-Rad, Hercules, CA, USA).

Osteoclast differentiation assay

Bone marrow cells were obtained by flushing femurs of 6-week-old female Lewis rats and were seeded at 2×10^7 cells per 10 cm Petri dish, then cultured in α -minimal essential medium containing 10% FCS and 1% penicillin/streptomycin. One day after the treatment, non-adherent cells were seeded again and cultured in α -minimal essential medium containing 10% FCS, 1% penicillin/streptomycin, and 20 ng/ml M-CSF in Lab-Tek eight-well chamber slides (Nalge Nunc, New York, NY, USA) at a density of 2×10^5 cells per well. Two days after the incubation, cells were cultured with 100 ng/ml RANKL and 20 ng/ml M-CSF for 7 days. On days 1, 3, and 5 various decoy ODNs were transiently transferred. Then the cells were washed and stained with a commercial TRAP staining kit (Cell

Figure 1



Structures and sequences of the decoy oligodeoxynucleotides used in this study. PNODN and RNODN (phosphorothionated decoy oligodeoxynucleotides) contain the NF- κ B-binding site in its double-stranded lesion (consensus sequences are underlined).

Garage, Tokyo, Japan). The number of TRAP-positive multinuclear (three or more nuclei) cells was counted.

Pit formation assay

To examine the effect of RNODN on resorbing activity, cells were cultured on BD BioCoat osteologic calcium hydroxyapatite-coated slides (BD Biosciences, Bedford, MA, USA) in a 5% CO₂ incubator. The non-adherent bone marrow cells were seeded at a density of 10⁵ cells per well. After incubation for 2 days with 20 ng/ml M-CSF, cells were cultured with 100 ng/ml RANKL and 20 ng/ml M-CSF. On days 3, 5, and 7 various decoy ODNs were transiently transferred, and on day 8 cells were washed vigorously and the calcified matrix resorption area on each disc was measured with a Mac SCOPE image analyzer, version 2.51 (Mitani, Fukui, Japan).

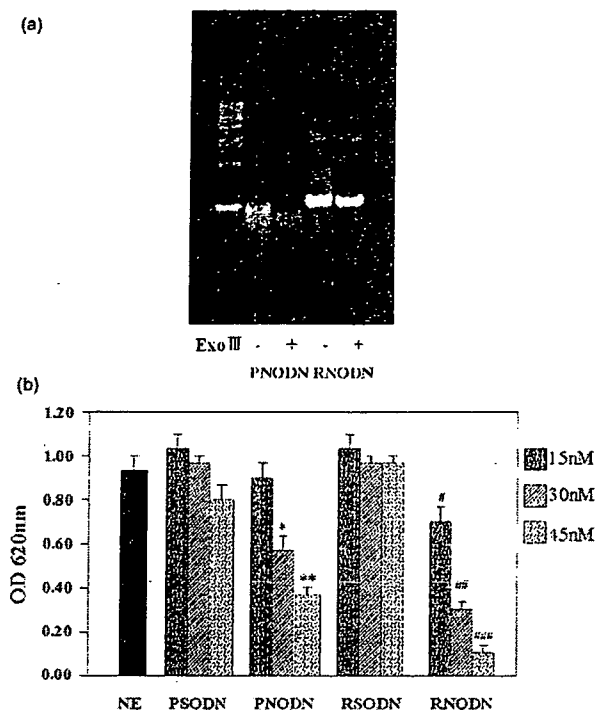
Immunofluorescence staining

Cells were fixed in 4% paraformaldehyde for 20 minutes at 37°C and treated with 0.5% Triton X-100 for 5 minutes. Cells were then blocked for 30 minutes with 2% goat serum/PBS and incubated in 4 μ g/ml rabbit polyclonal antibody against NFATc1 (sc-13033; Santa Cruz biotechnology, Santa Cruz, CA, USA) at 4°C for 16 hours and 400 ng/ml Alexa 488 goat anti-rabbit IgG (A-12373; Invitrogen Molecular Probes, Carlsbad, CA, USA) at room temperature for 60 minutes. The density of fluorescence was estimated by calculating the area of fluorescent cells by NIH image software.

Induction of arthritis by collagen in rats

This experimental study was performed in accordance with the recommendations in the Guide for the Care and Use of Laboratory Animals of National Institutes of Health (NIH). The protocol was approved by the committee on the Ethics of Animal Experiments in Osaka University. Arthritis was induced by col-

Figure 2



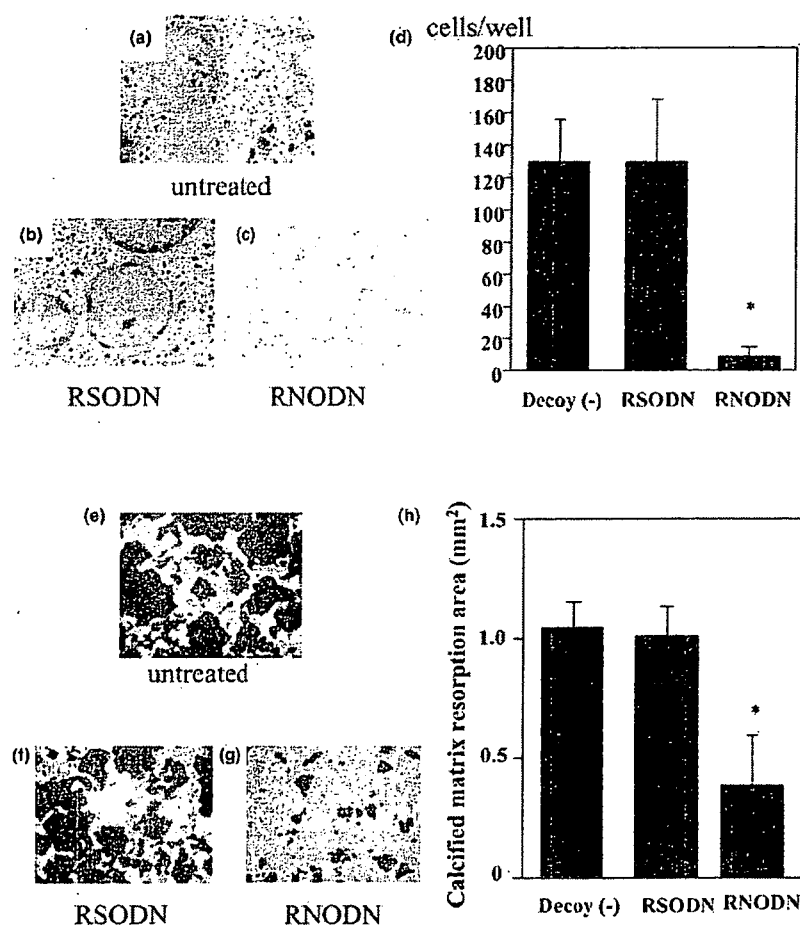
The stability and binding activity of RNODN and PNODN. (a) Stability of phosphorothionate double-stranded NF- κ B decoy oligodeoxynucleotide (PNODN) and ribbon-type NF- κ B decoy oligodeoxynucleotide (RNODN) in the presence of exonuclease III. (b) Effects of various decoys on binding activity towards NF- κ B. The binding activity of decoy oligodeoxynucleotides (ODNs) reflected their ability to decrease absorbance. NE, nuclear extract without treatment of decoy ODN. ($n = 5$ per group; * $p < 0.05$, ** $p < 0.01$, # $p < 0.05$, ## $p < 0.01$, ### $p < 0.001$ compared with nuclear extract without treatment of decoy ODN.)

lagen with the use of the modified method described by Trentham and colleagues [31]. In brief, 6-week-old female Lewis rats were immunized intradermally with 0.5 mg of bovine type II collagen, which was dissolved in 0.5 ml of 0.1 M acetic acid at 4°C and emulsified in 0.5 ml of cold Freund's incomplete adjuvant. On day 7, the rats received an intradermal booster injection of half the volume of the first immunization. Onset of arthritis in the ankle joints could be usually recognized visually between days 10 and 14. All rats in which the onset of arthritis could not be recognized visually by day 14 were excluded from this study.

In vivo transfer of fluorescein isothiocyanate (FITC)-labeled RNODN

To examine the localization of RNODN delivery, 50 μ g of FITC-labeled RNODN were injected intra-articularly. One day after transfer, synovial tissues were extracted and fixed. Cryostat sections of synovial cells were observed by ultraviolet microscopy (T6300; Nikon, Tokyo, Japan). The sections were also stained with 4',6-diamidino-2-phenylindole.

Figure 3



Osteoclast differentiation induced *in vitro* by macrophage colony-stimulating factor and RANKL. Cells were transiently transfected with ribbon-type scrambled decoy oligodeoxynucleotide (RSODN) (b) or ribbon-type NF- κ B decoy oligodeoxynucleotide (RNODN) (c), or were untreated alone (a). Original magnification $\times 100$. (d) Numbers of TRAP-positive multinuclear cells. ($n = 5$ per group; $*p < 0.001$, compared with rats treated with RSODN.) (e-h) Calcified matrix resorption by osteoclast-like cells induced by soluble receptor activator of nuclear factor κ B ligand (RANKL). Cells were transiently transfected with RSODN (f) or RNODN (g) or were untreated alone (e). (h) Mean calcified matrix resorption areas calculated by MacSCOPE image analyzer. ($n = 5$ per group; $*p < 0.01$ compared with the RSODN-treated group.)

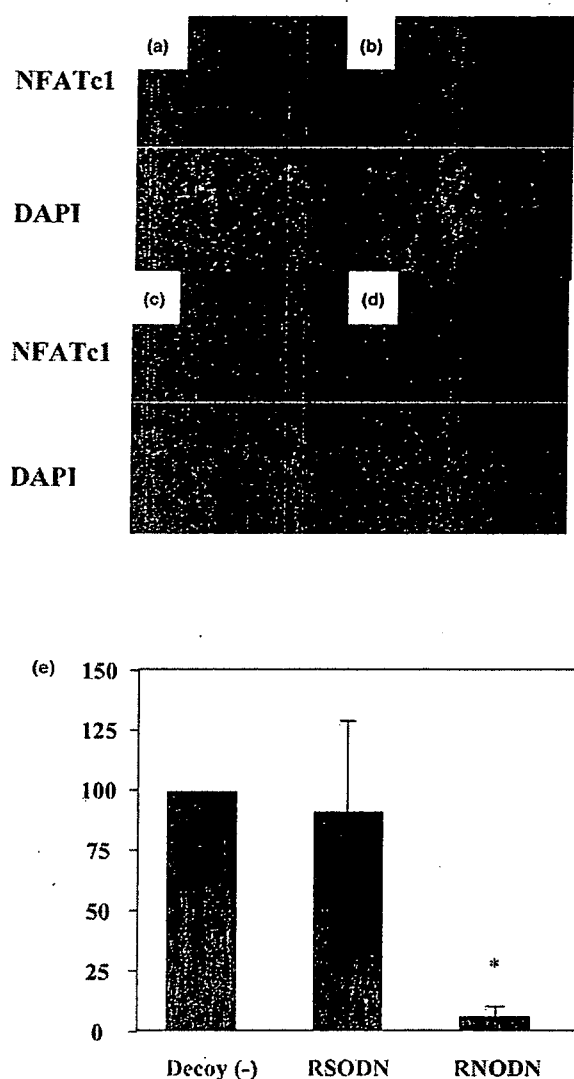
Experimental protocol

On day 14 after immunization, 50 μ l of suspension containing 200 μ g of RNODN or 200 μ g of RSODN or 50 μ l of PBS was administered intra-articularly with a 30-gauge needle into the right side hind-ankle joint of rats with collagen-induced arthritis (CIA). Administration was performed once every week for 3 weeks. At the end of the experiment (day 35), the ankle joints were fixed in 4% paraformaldehyde, decalcified with EDTA, and embedded in paraffin; sections 4 μ m thick were prepared. Next, sections were stained with hematoxylin and eosin. The extent of arthritis in the ankle joints was assessed in accordance with the method reported previously [32]: 0 = normal synovium, 1 = synovial membrane hypertrophy, 2 = pannus and cartilage erosion, 3 = major erosion of cartilage and subchondral bone, and 4 = loss of joint integrity and ankylosis.

To investigate the osteoclastic activity *in vivo*, sections were stained with a TRAP staining kit (Cell Garage, Tokyo, Japan). TRAP-positive multinuclear cells were counted in the sections of each ankle (at $\times 100$ magnification). All procedures complied with the standards described in the Osaka University Medical School Guidelines for the Care and Use of Laboratory Animals.

Statistical analysis

Statistical analysis was performed with the unpaired *t* test and the Mann-Whitney *U* test; $p < 0.05$ was considered significant. All experiments *in vitro* were performed at least three times.

Figure 4

Expression of NFATc1 protein in osteoclast precursor cells. (a-d) Immunohistochemistry of NFATc1 protein with specific antibody in osteoclast precursor cells. Bone marrow macrophages were incubated with M-CSF/RANKL for 48 hours after incubation with ribbon-type scrambled decoy oligodeoxynucleotide (RSODN) (c) or ribbon-type NF- κ B decoy oligodeoxynucleotide (RNODN) (d), or were untreated alone (b). (a) Without reaction with primary antibody. The expression of NFATc1 by immunofluorescence is shown in each upper panel. Nuclei stained with 4',6-diamidino-2-phenylindole are shown in each lower panel. Original magnification $\times 100$. (e) Measurement of fluorescent area of osteoclast precursor cells. The areas of fluorescent cells in RSODN-treated and RNODN-treated groups are shown as percentages over that of the untreated group. ($n = 5$ per group; * $p < 0.001$ compared with the RSODN-treated group.)

Results

Stability of RNODN

In this study we used RNODNs to improve stability to exonuclease. Initially, the structural stability of decoy ODN was

examined by the ability to resist degradation in the presence of exonuclease III. The primary cause of degradation of standard DNA oligomers in biological applications is a 3'-exonuclease activity found in cells [33,34]. RNODN showed high resistance to exonuclease III and was observed as a major band in gel electrophoresis. In comparison with RNODN, PNODN was degraded after incubation in the presence of exonuclease III (Figure 2a).

Binding activity of RNODNs on NF- κ B

To examine the binding activity of RNODN on the NF- κ B protein, an *in vitro* competition assay was performed with Mercury Transfactor Kits for NF- κ B p65 (Figure 2b). An increase in the concentration of unbound NF- κ B protein was accompanied by a corresponding increase in absorbance. The binding activity of decoy ODNs reflected their ability to decrease the absorbance level. The result of calculating the absorbance of each group is shown as a percentage over that of the untreated group. When PNODN or RNODN was used as a competitor oligonucleotide at 30 or 45 nM, a significant decrease in absorbance was confirmed against the absorbance of nuclear extract without competitor oligonucleotides. A stronger competitive effect was observed when RNODN was used than with PNODN. At a concentration of 15 nM, the competitive effect was observed only in the RNODN-treated group. When RSODN or PSODN was used as a competitor oligonucleotide, the decrease in absorbance was minimal compared with that of nuclear extract without competitor oligonucleotides. The result shows that RNODN has specific and strong binding activity on the NF- κ B protein.

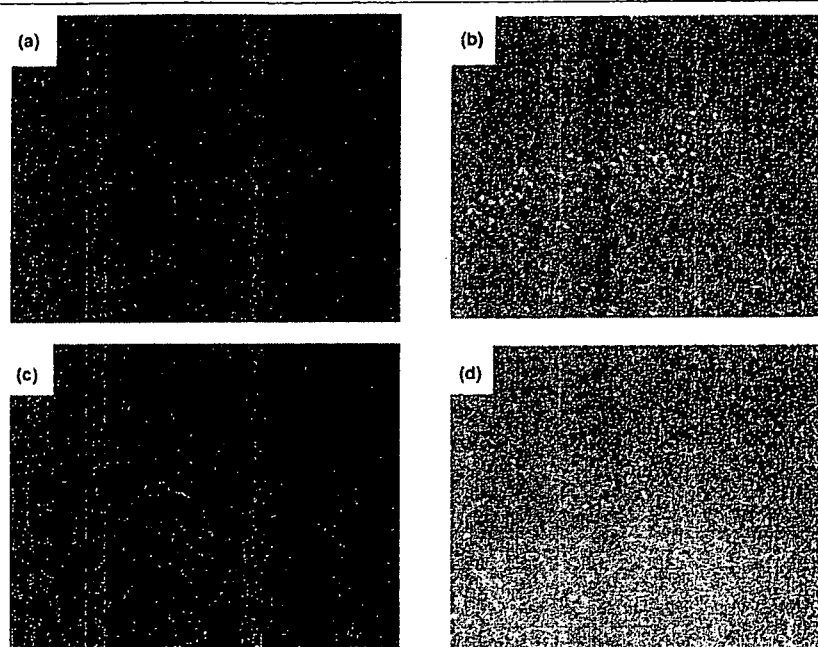
RNODN inhibits RANKL-induced osteoclastogenesis

To examine the effects of RNODN on osteoclastogenesis *in vitro*, bone marrow macrophages were incubated with decoy in the presence of RANKL and M-CSF (Figure 3a-c). The number of TRAP-positive multinuclear cells in the untreated group and in the RSODN-treated and RNODN-treated groups were 124.2 ± 34.6 , 126.2 ± 45.5 , and 5.2 ± 1.9 , respectively (mean \pm SD; Figure 3d). Osteoclastogenesis induced by RANKL was inhibited by incubation with RNODN ($p < 0.001$ compared with the RSODN-treated group). The inhibitory effect was not observed when cells were incubated with RSODN (Figure 3).

RNODN inhibits RANKL-induced pit formation

To examine the inhibitory effects of RNODN on the activation of osteoclasts, a pit formation assay was performed (Figure 3e-g). The calcified matrix resorption area in the untreated group and in the RSODN-treated and RNODN-treated groups were 1.03 ± 0.12 , 1.01 ± 0.12 , and 0.36 ± 0.21 mm², respectively (mean \pm SD; Figure 3h). Results showed that calcified matrix resorption by RANKL-induced osteoclast-like cells was significantly inhibited by incubation with RNODN ($p < 0.01$ compared with the RSODN-treated group). The inhibitory

Figure 5



Representative findings of fluorescence microscopy of synovium transferred with FITC-labeled RNODN. (a) Synovium transferred with ribbon-type NF- κ B decoy oligodeoxynucleotide (RNODN) not labeled with fluorescein isothiocyanate (FITC). (b) The sections were counterstained with 4',6-diamidino-2-phenylindole. (c) Synovium transferred with FITC-labeled RNODN. Original magnification \times 200. (d) The sections were counterstained with 4',6-diamidino-2-phenylindole.

effect was not observed when cells were incubated with RSODN.

Downregulation of NFATc1 by RNODN

To clarify the mechanism underlying the inhibitory effect of RNODN on osteoclastogenesis, we examined the expression of the NFATc1 protein in bone marrow cells incubated with RANKL. NFATc1 is a master switch for regulating the terminal differentiation of osteoclasts, functioning downstream of RANKL [35]. As shown in Figure 4, the expression of NFATc1 in RANKL-stimulated bone marrow cells increased in accordance with the fusion of cells (Figure 4b). The results of calculating the area of fluorescent cells in RSODN-treated and RNODN-treated groups are shown as percentages over that of the untreated group. The data for each group (mean \pm SD) are $90.0 \pm 38.6\%$ and $3.5 \pm 3.2\%$, respectively (Figure 4e). The expression of NFATc1 was inhibited by incubation with RNODN ($p < 0.001$ compared with the RSODN-treated group; Figure 4d).

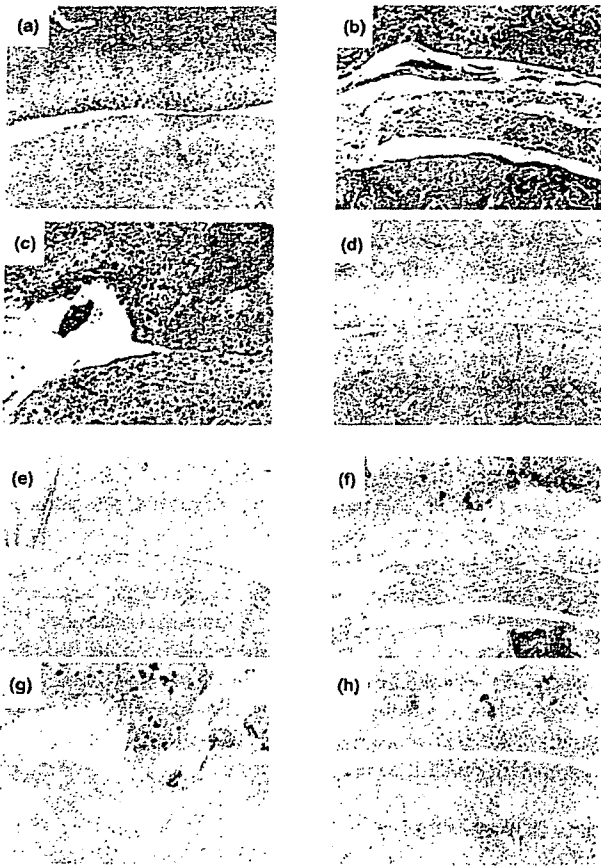
In vivo transfer of FITC-labeled RNODN into joint synovium

We performed *in vivo* transfer of FITC-labeled RNODN into rat ankle joints. Fluorescence was localized in synovial cells, especially the surface area (Figure 5c). Synovium transferred with decoy ODN not labeled with FITC showed no specific flu-

orescence (Figure 5a). The nucleus was stained with 4',6-diamidino-2-phenylindole (Figure 5b,d).

Inhibitory effects of intra-articular injection of RNODN on joint destruction and osteoclast activity in rats with CIA

To evaluate the effect of RNODN on joint destruction and osteoclast activation, we performed a histological analysis of the ankle joints treated with RNODN, RSODN, or PBS. Histologically, ankle joints of rats with CIA treated with PBS (Figure 6b) or RSODN (Figure 6c) showed pannus invasion and massive cellular infiltration of the synovium, with disruption of cartilage and subchondral bone. Conversely, ankle joints of rats with CIA treated with RNODN (Figure 6d) showed marked improvement in arthritis. The arthritis scores (mean \pm SD) of PBS-treated joints, RSODN-treated joints, and RNODN-treated joints were 3.0 ± 0.7 , 3.2 ± 0.8 , and 1.8 ± 0.8 , respectively (Table 1). The number of osteoclasts around the ankle joints was significantly smaller in RNODN-treated rats than in RSODN-treated or PBS-treated rats (Figure 6f,g). The numbers of osteoclasts in PBS-treated joints, RSODN-treated joints, and RNODN-treated joints were 142.8 ± 15.1 , 153.8 ± 28.2 , and 31.0 ± 27.3 , respectively (Table 1). Figure 6a and Figure 6e show HE staining and TRAP staining of ankle joints in naive rats.

Figure 6

Histological analysis in the ankle joints of rats with collagen-induced arthritis (CIA) at day 35. Samples were stained with hematoxylin and eosin in (a-d) and with tartrate-resistant acid phosphatase [TRAP] in (e-h). (a) Naive rats had normal joints. (b) Ankle joints of rats with CIA treated with PBS showed pannus invasion and massive cellular infiltration of the synovium, with disruption of cartilage and subchondral bone. (c) Ankle joints of rats with CIA treated with ribbon-type scrambled decoy oligodeoxynucleotide (RSODN) also showed pannus invasion and massive cellular infiltration of the synovium, with disruption of cartilage and subchondral bone. (d) Ankle joints of rats with CIA treated with ribbon-type NF- κ B decoy oligodeoxynucleotide (RNODN) also had nearly intact articular joints. (e) Ankle joints of naive rats had few TRAP-positive multinuclear cells. (f) Ankle joints of rats with CIA treated with PBS showed active resorption of cartilage and subchondral bone by pannus and synovium including TRAP-positive multinuclear cells. (g) Ankle joints of rats with CIA treated with RSODN also showed active resorption of cartilage and subchondral bone by pannus and synovium including TRAP-positive multinuclear cells. (h) TRAP-positive multinuclear cell formation was suppressed in ankle joints of rats with CIA treated with RNODN. Original magnifications \times 100.

Discussion

The Rel/NF- κ B family of transcription factors is induced in response to several signals. In unstimulated cells, NF- κ B is associated in the cytoplasm with the inhibitory protein I κ B. In response to an external signal, I κ B is phosphorylated and degraded, releasing NF- κ B to enter the nucleus and activate

transcription [36,37]. The wide variety of genes regulated by NF- κ B includes cytokines, chemokines, adhesion molecules, acute-phase proteins, and inducible effector enzymes. The important role of NF- κ B in the differentiation and activation of osteoclasts has been mentioned previously [38]. Selective inhibition of NF- κ B by several drugs blocks osteoclastogenesis [11,12]. In the present study we have shown that selective inhibition of NF- κ B with a ribbon-type NF- κ B decoy could suppress the differentiation and activation of RANKL-induced osteoclastogenesis. Transfection of decoy ODN corresponding to the *cis* sequences result in the attenuation of authentic *cis-trans* interaction, leading to the removal of *trans*-factors from the endogenous *cis*-element, with subsequent modulation of gene expression [39]. The principle of the transcription factor decoy approach is based on the reduction of promoter activity as a result of the inhibition of binding of a transcription factor to a specific sequence in the promoter region. This approach is relatively simple and can be targeted to specific tissues; decoy ODN can be more effective than antisense ODN in blocking constitutively expressed factors as well as multiple transcription factors that bind to the same *cis* element [39]. However, one of the major limitations of the decoy ODN approach is the rapid degradation of phosphodiester ODN by intracellular nucleases [40-42]. The lack of sequence specificity of phosphodiester ODN has been reported previously [29,43,44]. To overcome these issues, the circular dumbbell double-stranded decoy ODN was developed [42,45,46]. Circular dumbbell decoy ODN for AP-1 or E2F have been demonstrated to be more effective than conventional decoy ODN in previous studies [40,41]. In this study, RNODN showed higher resistance to exonuclease and stronger binding activity on NF- κ B than PNODN, and we examined the effect of RNODN for the inhibition of osteoclast differentiation and activation. A previous report [47] showed the effect of decoy targeting NF- κ B on apoptosis of human osteoclasts. In contrast to their results we were unable to show the specific effect of RNODN for apoptosis of rat osteoclasts. It is not yet clear whether NF- κ B is responsible for the survival of osteoclasts [48].

In this study, we were able to transfer decoy ODN to adherent macrophage/monocyte-like cells and osteoclast-like cells without reagent. The possibility and effectiveness of ODN transfer into these cells have been reported previously [49]. The cellular uptake of ODN is reportedly achieved by a receptor-mediated endocytosis mechanism [50,51]. However, the exact mechanism of cellular uptake of naked DNA or ODN is still poorly defined [52]. The efficiency of internalizing naked DNA varies between cell types [52]. In our study, the effectiveness of ODN transfer was promoted in serum-free conditions. The size of the ribbon-type decoy is about 20 base pairs, which is small compared with the plasmid, so it may be easier for ODN to be transferred into osteoclasts or their precursors.

Table 1**Mean histological scores and osteoclast numbers of rats with collagen-induced arthritis**

Group	Number of joints	Histological score	Osteoclast number
PBS injection	5	3.0 ± 0.7	142.8 ± 15.1
RSODN injection	5	3.2 ± 0.8	153.8 ± 28.2
RNODN injection	5	1.8 ± 0.8 ^a	31.0 ± 37.3 ^b

^a*p* < 0.01 compared with PBS injection group; ^b*p* < 0.01 compared with PBS-injection group (*n* = 5 rats and *n* = 5 joints for each group). RNODN, ribbon-type NF-κB decoy oligodeoxynucleotide; RSODN, ribbon-type scrambled decoy oligodeoxynucleotide. Results are means ± SD.

In the pit formation assay of this study, we transferred the decoy on day 3. We were able to confirm TRAP-positive multinuclear cells on day 3 but the cells were not so large and it might be difficult to state that these cells were mature osteoclasts. It would have been better if we could have incubated mature osteoclasts on a hydroxyapatite-coated disc, but osteoclasts are easily damaged and it is technically difficult to subculture rat mature osteoclasts.

In the previous study, the gene encoding NFATc1, a member of the NFAT family of transcription factor genes, was found to be the most strongly induced transcription factor gene after stimulation by RANKL in osteoclast differentiation. NFATc1 autoamplifies its own gene, possibly by binding to its own promoter [35]. The AP-1 and NF-κB binding sites are present with the promoter region of the NFATc1 gene [53]. Recently, Takatsuna and colleagues showed that (-)-DHMEQ, a newly designed NF-κB inhibitor, inhibited RANKL-induced osteoclast differentiation in mouse bone marrow macrophages through the downregulation of NFATc1 [54]. In the present study the expression of NFATc1 was inhibited by treatment with RNODN.

The skeletal complications of RA consist of focal bone erosions and periarticular osteoporosis at sites of active inflammation, and generalized bone loss with reduced bone mass. In rheumatoid synovium, activated T cells and fibroblasts express RANKL. TNF-α and IL-1β are also overproduced in synovium. TNF-α and IL-1β, acting in concert with RANKL, can powerfully promote osteoclast recruitment, activation, and osteolysis in RA [55]. In the synovium of patients with RA, NF-κB was present in most macrophages within the lining and sublining lesions throughout the synovium, including endothelial cells [56,57]. CIA is an autoimmune model that in many ways resembles RA. Immunization of genetically susceptible rodents with type II collagen leads to the development of severe polyarticular arthritis mediated by an autoimmune response. Just as in RA, synovitis and erosions of cartilage and bone are hallmarks of CIA [58]. In the present study, direct injection of RNODN in arthritic joints of rats with CIA led to an amelioration of arthritis and decreased the number of TRAP-

positive cells in the synovium. The strategy of naked RNODN transfer into the joint implies a potential for future clinical treatment.

Conclusion

RNODN showed higher resistance to exonuclease and higher binding activity on NF-κB than did PNODN. Differentiation and calcium resorption were suppressed by treatment with RNODN, by preventing NFATc1 expression. Joint destruction and osteoclast activity were significantly suppressed by intra-articular injection of RNODN.

These data suggest that RNODNs inhibit the induction and activity of osteoclasts and that the direct injection of RNODNs into the joints might be an effective strategy for the treatment of arthritis.

Competing interests

The authors declare that they have no competing interests.

Authors' contributions

YK performed molecular and animal experiments, measurements and evaluation of the data, and statistical analyses. TT supervised the study design, the interpretation of data, and the writing of the manuscript. TN conceived and participated in the experimental design of the study. RM and HY supervised the study design and gave valuable advice to YK. All authors read and approved the final manuscript.

Additional files

The following Additional files are available online:

Additional File 1

A PDF containing a supplementary figure that demonstrates that there is no activity in the nuclear extracts leading to time-dependent degradation of DNA. See <http://www.biomedcentral.com/content/supplementary/ar1980-S1.pdf>

Additional File 2

A PDF containing a supplementary figure that examines the effects of RSODN and RNODN on cell growth. See <http://www.biomedcentral.com/content/supplementary/ar1980-S2.pdf>

Acknowledgements

We wish to thank Tsuyoshi Tajima, Hideaki Sato, and Masafumi Yoshino for their excellent technical assistance. This study was supported in part by grants from the Ministry of Education, Culture, Sports, Science, and Technology of Japan, and the Ministry of Health, Labour and Welfare of Japan.

References

1. Teitelbaum SL: Bone resorption by osteoclasts. *Science* 2000, **289**:1504-1508.
2. Yasuda H, Shima N, Nakagawa N, Yamaguchi K, Kinosaki M, Goto M, Mochizuki SI, Tsuda E, Morinaga T, Udagawa N, et al.: A novel molecular mechanism modulating osteoclast differentiation and function. *Bone* 1999, **25**:109-113.
3. Suda T, Takahashi N, Udagawa N, Jimi E, Gillespie MT, Martin TJ: Modulation of osteoclast differentiation and function by the new members of the tumor necrosis factor receptor and ligand families. *Endocr Rev* 1999, **20**:345-357.
4. Yao GQ, Sun BH, Hammond EE, Spencer EN, Horowitz MC, Insogna KL, Weir EC: The cell-surface form of colony-stimulating factor-1 is regulated by osteotropic agents and supports formation of multinucleated osteoclast-like cells. *J Biol Chem* 1998, **273**:4119-4128.
5. Shigeyama Y, Pap T, Kunzler P, Simmen BR, Gay RE, Gay S: Expression of osteoclast differentiation factor in rheumatoid arthritis. *Arthritis Rheum* 2000, **43**:2523-2530.
6. Kong YY, Yoshida H, Sarosi I, Tan HL, Timms E, Capparelli C, Morony S, Oliveira-dos-Santos AJ, Van G, Itie A, et al.: OPGL is a key regulator of osteoclastogenesis, lymphocyte development and lymph-node organogenesis. *Nature* 1999, **397**:315-323.
7. Hsu H, Lacey DL, Dunstan CR, Solovyev I, Colombero A, Timms E, Tan HL, Elliott G, Kelley MJ, Sarosi I, et al.: Tumor necrosis factor receptor family member RANK mediates osteoclast differentiation and activation induced by osteoprotegerin ligand. *Proc Natl Acad Sci USA* 1999, **96**:3540-3545.
8. Lacey DL, Timms E, Tan HL, Kelley MJ, Dunstan CR, Burgess T, Elliott R, Colombero A, Elliott G, Scully S, et al.: Osteoprotegerin ligand is a cytokine that regulates osteoclast differentiation and activation. *Cell* 1998, **93**:165-176.
9. Wei S, Teitelbaum SL, Wang MW-H, Ross FP: Receptor activator of nuclear factor- κ B ligand activates nuclear factor- κ B in osteoclast precursors. *Endocrinology* 2001, **142**:1290-1295.
10. Boyce BF, Xing L, Franzoso G, Siebenlist U: Required and non-essential functions of nuclear factor- κ B in bone cells. *Bone* 1999, **25**:137-139.
11. Jimi E, Aoki K, Saito H, Acquisto FD, May MJ, Nakamura I, Sudo T, Kojima T, Okamoto F, Fukushima H, et al.: Selective inhibition of NF- κ B blocks osteoclastogenesis and prevents inflammatory bone destruction *in vivo*. *Nat Med* 2004, **10**:617-624.
12. Bharti AC, Takada Y, Aggarwal BB: Curcumin (diferuloylmethane) inhibits receptor activator of NF- κ B ligand-induced NF- κ B activation in osteoclast precursors and suppresses osteoclastogenesis. *J Immunol* 2004, **172**:5940-5947.
13. Franzoso G, Carlson L, Xing L, Poljak L, Shores EW, Brown KD, Leonardi A, Tran T, Boyce BF, Siebenlist U: Requirement for NF- κ B in osteoclast and B-cell development. *Genes Dev* 1997, **11**:3482-3496.
14. Iotsova V, Caamano J, Loy J, Yang Y, Lewin A, Bravo R: Osteopetrosis in mice lacking NF- κ B1 and NF- κ B2. *Nat Med* 1997, **3**:1285-1289.
15. Ruocco MG, Maeda S, Park JM, Lawrence T, Hsu LC, Cao Y, Schett G, Wagner EF, Karin M: I κ B kinase (IKK) β but not IKK α , is a critical mediator of osteoclast survival and is required for inflammation-induced bone loss. *J Exp Med*. 2005, **201**:1677-1687.
16. Takayanagi H, Oda H, Yamamoto S, Kawaguchi H, Tanaka S, Nishikawa T, Koshihara Y: A new mechanism of bone destruction in rheumatoid arthritis: Synovial fibroblasts induce osteoclastogenesis. *Biochem Biophys Res Commun* 1997, **240**:279-286.
17. Takano H, Tomita T, Totosaki-Maeda T, Maeda-Taniyama M, Tsuboi H, Takeuchi E, Kaneko M, Shi K, Takahi K, Myoui H, et al.: Comparison of the activities of multinucleated bone-resorbing giant cells derived from CD14-positive cells in the synovial fluids of rheumatoid arthritis and osteoarthritis patients. *Rheumatology* 2004, **43**:435-441.
18. Gravallesse EM, Harada Y, Wang JT, Gorn AH, Thornhill TS, Goldring SR: Identification of cell types responsible for bone resorption in rheumatoid arthritis and juvenile rheumatoid arthritis. *Am J Pathol* 1998, **152**:943-951.
19. Lubberts E, Oppers-Walgreen B, Pettit AR, Bertselaar L, Joosten L, Goldring SR, Gravallesse EM, Berg WB: Increase in expression of receptor activator of nuclear factor κ B, at sites of bone erosion correlates with progression of inflammation in evolving collagen-induced arthritis. *Arthritis Rheum* 2002, **46**:3055-3064.
20. Pettit AR, Ji H, von Stechow D, Muller R, Goldring SR, Choi Y, Benoist C, Gravallesse EM: TRANCE/RANKL knockout mice are protected from bone erosion in a serum transfer model of arthritis. *Am J Pathol* 2001, **159**:1689-1699.
21. Mann MJ, Dzau VJ: Therapeutic application of transcriptional factor decoy oligonucleotides. *J Clin Invest* 2000, **106**:1071-1075.
22. Dzau VJ: Transcription factor decoy. *Circ Res* 2002, **90**:1234-1236.
23. Morishita R, Sugimoto T, Aoki M, Kida I, Tomita N, Moriguchi A, Maeda K, Sawa Y, Kaneda Y, Higaki J, et al.: *In vivo* transfection of cis element 'decoy' against nuclear factor- κ B binding site prevents myocardial infarction. *Nat Med* 1997, **3**:894-899.
24. Tomita T, Takeuchi E, Tomita N, Morishita R, Kaneko M, Yamamoto K, Nakase T, Seki H, Kato K, Kaneda Y, et al.: Suppressed severity of collagen-induced arthritis by *in vivo* transfection of nuclear factor- κ B decoy oligodeoxynucleotides as a gene therapy. *Arthritis Rheum* 1999, **42**:2532-2542.
25. Tomita T, Takano H, Tomita N, Morishita R, Kaneko M, Shi K, Takahi T, Nakase Y, Kaneda Y, Yoshikawa H, Ochi T: Transcription factor decoy for NF κ B inhibits cytokine and adhesion molecule expressions in synovial cells derived from rheumatoid arthritis. *Rheumatology* 2000, **39**:749-757.
26. Tomita N, Morishita R, Tomita S, Yamamoto K, Aoki M, Matsushita H, Hayashi S, Higaki J, Ogihara T: Transcription factor decoy for nuclear factor- κ B inhibits tumor necrosis factor- α -induced expression of interleukin-6 and intracellular adhesion molecule-1 in endothelial cells. *J Hypertens* 1998, **16**:993-1000.
27. Lee IK, Ahn JD, Kim HS, Park JY, Lee KU: Advantages of the circular dumbbell decoy in gene therapy and studies of gene regulation. *Curr Drug Targets* 2003, **4**:619-623.
28. Tomita N, Tomita T, Yuyama K, Tougan T, Tajima T, Ogihara T, Morishita R: Development of novel decoy oligonucleotides: advantages of circular dumb-bell decoy. *Curr Opin Mol Ther* 2003, **5**:107-112.
29. Hosoya T, Takeuchi H, Kanesaka Y, Yamakawa H, Miyano-Kurosaki N, Takai K, Yamamoto N, Takaku H: Sequence-specific inhibition of a transcription factor by circular dumbbell DNA oligonucleotides. *FEBS Lett* 1999, **461**:136-140.
30. Moon IJ, Choi K, Choi YK, Kim JE, Lee Y, Schreiber AD, Park JG: Potent growth inhibition of leukemic cells by novel ribbon-type antisense oligonucleotides to c-myc1. *J Biol Chem* 2000, **275**:4647-4653.
31. Trentham D, Townes A, Kang A: Autoimmunity to type 2 collagen: an experimental model of arthritis. *J Exp Med* 1977, **146**:857-868.
32. Shiozawa S, Shimizu K, Tanaka K, Hino K: Studies on the contribution of c-fos/AP-1 to arthritic joint destruction. *J Clin Invest* 1997, **99**:1210-1216.
33. Rumney SIV, Kool ET: DNA recognition by hybrid oligoether-oligodeoxynucleotide macrocycles. *Angew Chem Int Ed Engl* 1992, **31**:1617-1619.
34. Gamper HB, Reed MW, Cox T, Viroso JS, Adams AD, Gall AA, Scholler JK, Meyer RB Jr: Facile preparation of nuclease resistant 3' modified oligodeoxynucleotides. *Nucleic Acids Res* 1993, **21**:145-150.
35. Takayanagi H, Kim S, Koga T, Nishina H, Isshiki M, Yoshida H, Saiura A, Isobe M, Yokochi T, Inoue J, et al.: Induction and activation of the transcription factor NFATc1(NFAT2) integrate RANKL signaling in terminal differentiation of osteoclasts. *Dev Cell* 2002, **3**:889-901.
36. Verma IM, Stevenson JK, Schwarz EM, Van Antwerp D, Miyamoto S: Rel/NF- κ B/I κ B family: intimate tales of association and dissociation. *Genes Dev* 1995, **9**:2723-2735.
37. Karin M, Delhase M: The I κ B kinase (IKK) and NF- κ B: key elements of proinflammatory signaling. *Immunology* 2000, **12**:85-98.
38. Jimi E, Nakamura I, Ikebe T, Akiyama S, Takahashi N, Suda T: Activation of NF- κ B is involved in the survival of osteoclasts promoted by interleukin-1. *J Biol Chem* 1998, **273**:8799-8805.
39. Morishita R, Tomita N, Kaneda Y, Ogihara T: Molecular therapy to inhibit NF κ B activation by transcription factor decoy oligonucleotides. *Curr Opin Pharmacol* 2004, **4**:139-146.

40. Ahn JD, Morishita R, Kaneda Y, Lee SJ, Kwon KY, Choi SY, Lee KU, Park JY, Moon IJ, Park JG, et al.: Inhibitory effects of novel AP-1 decoy oligodeoxynucleotides on vascular smooth muscle cell proliferation *in vitro* and neointimal formation *in vivo*. *Circ Res* 2002, **90**:1325-1332.
41. Ahn JD, Morishita R, Kaneda Y, Kim HS, Chang Y-C, Lee K-U, Kim YH, Lee IK: Novel E2F decoy oligodeoxynucleotides inhibit *in vitro* vascular smooth muscle cell proliferation and *in vivo* neointimal hyperplasia. *Gene Ther* 2002, **9**:1682-1692.
42. Park KK, Ahn JD, Lee IK, Magae J, Heintz NH, Kwak JY, Lee YC, Cho YS, Kim HC, Chae YM, et al.: Inhibitory effects of novel E2F decoy oligodeoxynucleotides on mesangial cell proliferation by coexpression of E2F/DP. *Biochem Biophys Res Commun* 2003, **308**:689-697.
43. Brown DA, Kang SH, Gryaznov SM, Dedionisio L, Heidenreich O, Sullivan S, Xu X, Nerenberg MI: Effect of phosphorothionate modification of oligodeoxynucleotides on specific protein binding. *J Biol Chem* 1994, **269**:26801-26805.
44. Khaled Z, Benimetskaya L, Zeltser R, Khan T, Sharma HW, Narayanan R, Stein CA: Multiple mechanisms may contribute to the cellular anti-adhesive effects of phosphorothionate oligodeoxynucleotides. *Nucleic Acids Res* 1996, **24**:737-745.
45. Chu BCF, Orgel LE: The stability of different forms of double-stranded decoy DNA in serum and nuclear extracts. *Nucleic Acids Res* 1992, **20**:5857-5858.
46. Chu BCF, Orgel LE: Binding of hairpin and dumbbell DNA to transcription factors. *Nucleic Acids Res* 1991, **19**:6958.
47. Penolazzi L, Lambertini E, Borgatti M, Piva R, Cozzani M, Giovannini I, Naccari R, Siciliani G, Gambari R: Decoy oligodeoxynucleotides targeting NF- κ B transcriptional factors: induction of apoptosis in human primary osteoclasts. *Biochem Pharmacology* 2003, **66**:1189-1198.
48. Miyazaki T, Katagiri H, Kanegae Y, Takayanagi H, Sawada Y, Yamamoto A, Pando MP, Asano T, Verma IM, Oda H, et al.: Reciprocal role of ERK and NF- κ B pathways in survival and activation of osteoclasts. *J Cell Biol* 2000, **148**:333-342.
49. Ishikawa T, Kamiyama M, Tani-ishi N, Suzuki H, Ichikawa Y, Hamaguchi Y, Momiyama N, Shimada H: Inhibition of osteoclast differentiation and bone resorption by cathepsin K antisense oligonucleotides. *Mol Carcinog* 2001, **32**:84-91.
50. Yakubov LA, Deeva EA, Zarytova VF, Ivanova EM, Rytte AS, Yurchenko LV, Vlassov VV: Mechanism of oligonucleotide uptake by cells: involvement of specific receptors? *Proc Natl Acad Sci USA* 1989, **86**:6454-6458.
51. Loke SL, Stein CA, Zhang XH, Mori K, Nakanishi M, Subasinghe C, Cohen JS, Neckers LM: Characterization of oligonucleotide transport into living cells. *Proc Natl Acad Sci USA* 1989, **86**:3474-3478.
52. Wu-Pong S: Alternative interpretations of the oligonucleotide transport literature: insights from nature. *Adv Drug Deliv Rev* 2000, **44**:59-70.
53. Zhou B, Cron RQ: Regulation of the murine Nfatc1 gene by NFATc2. *J Biol Chem* 2002, **277**:10704-10711.
54. Takatsuna H, Asagiri M, Kubota T, Oka K, Osada T, Sugiyama C, Saito H, Aoki K, Ohya K, Takayanagi H, et al.: Inhibition of RANKL-induced osteoclastogenesis by (-)-DHMEQ, a novel NF- κ B inhibitor, through downregulation of NFATc1. *J Bone Miner Res* 2005, **20**:653-662.
55. Romas E, Gillespie MT, Martin TJ: Involvement of receptor activator of NF- κ B ligand and tumor necrosis factor- α in bone destruction in rheumatoid arthritis. *Bone* 2002, **30**:340-346.
56. Marok R, Winyard PG, Coumbe A, Kus ML, Gaffney K, Blades S, Mapp PI, Morris CJ, Blake DR, Kaltschmidt C, et al.: Activation of the transcription factor nuclear factor- κ B in human inflamed synovial tissue. *Arthritis Rheum* 1996, **39**:583-591.
57. Handel ML, McMorrow LB, Gravalles EM: Nuclear factor- κ B in rheumatoid synovium. *Arthritis Rheum* 1995, **38**:1762-1770.
58. Myers LK, Rosloniec EF, Cremer MA, Kang AH: Collagen-induced arthritis, an animal model of autoimmunity. *Life Sci* 1997, **61**:1861-1878.

ORIGINAL ARTICLE

Takuma Matsubara · Akira Myoui · Fumiyo Ikeda
Kenji Hata · Hideki Yoshikawa · Riko Nishimura
Toshiyuki Yoneda

Critical role of cortactin in actin ring formation and osteoclastic bone resorption

Received: January 4, 2006 / Accepted: March 29, 2006

Abstract Tyrosine kinase c-Src plays an essential role in ruffled border formation and bone resorption in osteoclasts; however, it is unclear how c-Src controls ruffled border formation during bone resorption. To address this question, we investigated the role of cortactin, a c-Src substrate, in osteoclasts. We found that cortactin showed colocalization with c-Src and actin rings in osteoclasts. Overexpression of cortactin stimulated actin ring formation in RAW 264.7 cells. In contrast, overexpression of Csk inhibited tyrosine phosphorylation of cortactin and binding of cortactin to c-Src. More importantly, overexpression of a mutant cortactin strongly suppressed actin ring formation and bone resorbing activity in osteoclasts. Collectively, our data indicate that cortactin controls osteoclastic bone resorption by regulating actin organization.

Key words cortactin · c-Src · osteoclast

Introduction

A tyrosine kinase, c-Src, plays a critical role in actin organization and cytoskeletal structure [1]. Mice deficient in the *c-Src* gene manifest an osteopetrotic phenotype due to disorder of the ruffled border formation that is essential for osteoclastic bone resorption [2,3]. Consistent with these *in vivo* findings, osteoclasts isolated from *c-Src*-deficient mice fail to form actin rings, which are structures corresponding to the clear zone [4,5]. These findings suggest that c-Src regulates actin organization and exhibits an essential role in the bone resorbing activity of osteoclasts. However, the

molecular mechanisms by which c-Src controls bone resorption in osteoclasts is unknown.

Cortactin has been identified as a c-Src substrate [6]. Cortactin regulates actin polymerization by activating the actin-related protein2/3 (Arp2/3) complex and stabilizes the cortical actin network [7]. Recently, Arp2/3 was shown to be required for actin ring formation in osteoclasts [8]. We, therefore, speculated that cortactin is implicated in regulation of osteoclastic bone resorption as a downstream signaling molecule for c-Src. We found that cortactin shows almost identical localization with actin rings in osteoclasts. Furthermore, overexpression of mutant cortactin impaired actin ring formation and the bone resorbing activity of osteoclasts. Our findings support the proposition that cortactin conducts actin organization in osteoclasts and is required for osteoclastic bone resorption.

Materials and methods

Cell and reagents

A monocytic cell line, RAW 264.7, was purchased from the RIKEN cell bank (Tsukuba, Ibaraki, Japan) and cultured in minimum essential medium eagle, alpha modification (α -MEM) containing 10% fetal calf serum (FCS) (Valley Biomedical, Winchester, VA, USA). Soluble receptor activator of NF-kappaB ligand (sRANKL) and macrophage colony-stimulating factor (M-CSF) were purchased from Pepro-Tech EC (Rocky Hill, NJ, USA) and Green Cross (Osaka, Japan), respectively. Anti-c-Src and anticortactin antibodies were purchased from Oncogene Science (Cambridge, MA, USA) and Upstate Biotechnology (Lake Placid, NY, USA), respectively. 4,6 diamidino-2-phenylindole (DAPI) was purchased from Molecular Probes (Eugene, OR, USA) and rhodamine-labeled phalloidin from Fluka (St. Louis, MI, USA). c-Src and cortactin cDNA were kindly donated by Drs. Harold E. Varmus and Thomas Parsons. To generate a mutant cortactin lacking the actin binding domain, PCR products were synthesized and then subcloned into

T. Matsubara · F. Ikeda · K. Hata · R. Nishimura (✉) · T. Yoneda
Department of Molecular and Cellular Biochemistry, Graduate
School of Dentistry, Osaka University, 1-8 Yamadaoka, Suita
565-0871, Japan
Tel. +81-6-6879-2887; Fax +81-6-6879-2890
e-mail: rikonisi@dent.osaka-u.ac.jp

A. Myoui · H. Yoshikawa
Department of Orthopaedics, Graduate School of Medicine, Osaka
University, Osaka, Japan

pcDNA3 (Invitrogen, Carlsbad, CA, USA) and tagged with a Flag epitope at the N-terminus. The sequence of the construct was confirmed by DNA sequence analysis.

Osteoclast differentiation *in vitro*

Bone marrow cells or spleen cells were isolated from C57BL/6 mice (Nihon SLC, Hamamatsu, Shizuoka, Japan) and incubated with M-CSF (30 ng/ml) and sRANKL (100 ng/ml) for 6 days. After 6 days, the cells were analyzed by tartrate-resistant acid phosphate (TRAP) staining, and TRAP-positive multinucleated cells were counted as osteoclasts. RAW 264.7 cells were incubated in the presence of sRANKL (20 ng/ml) for 4 days.

Pit formation assay

To examine the function of TRAP-positive cells derived from spleen cells or bone marrow cells, we induced osteoclast formation on dentin slices. After 6 days of culture, cells were removed from the dentin slices. The resorption pits formed on dentine slices were stained with toluidine blue. The pit formation areas were quantified using an image analysis system, Image-Pro Plus (Silver Spring, MD, USA).

Immunoprecipitation and immunoblotting analysis

The cells were washed three times with ice-cold phosphate-buffered saline (PBS) and solubilized in lysis buffer [20 mM 2-[4-(2-Hydroxyethyl)-1-piperazinyl]ethanesulfonic acid (Hepes) (pH 7.4), 150 mM NaCl, 1 mM ethyleneglycol bis (2-aminoethylether)tetraacetic acid (EGTA), 1.5 mM MgCl₂, 10% glycerol, 1% Triton X-100, 10 µg/ml aprotinin, 10 µg/ml leupeptin, 1 mM phenylmethylsulfonyl fluoride (PMSF), and 0.2 mM sodium orthovanadate]. The lysates were centrifuged for 15 min at 4°C at 16000g and incubated with antibodies for 4 h at 4°C, followed by immunoprecipitation with protein A-sepharose (Zymed, CA, USA) or protein G-agarose (Boehringer Mannheim, Ingelheim, Germany). Immunoprecipitates were washed five times with lysis buffer and boiled in sodium dodecyl sulfate (SDS) sample buffer containing 0.5 M beta-mercaptoethanol; supernatants were recovered as immunoprecipitate samples. The immunoprecipitates or proteins isolated from RAW 264.7 cells were loaded for sodium dodecyl sulfate-polyacrylamide gel electrophoresis (SDS-PAGE) and immunoblotting was performed using specific antibodies. In all immunoblotting analyses, we also confirmed that equal amounts of proteins were loaded by staining the transferred membrane with Ponceau S.

Generation of adenovirus

The recombinant adenoviruses carrying c-Src, wild-type, or mutant cortactin were constructed by recombination between the expression cosmid cassette and the parental virus genome in 293 cells as previously described [9]. The viruses

were confirmed to retain no proliferative activity in the cells other than the 293 cells. Titers of the viruses were determined using the modified point assay [9].

Immunocytochemistry

Cells were washed three times with ice-cold PBS, fixed with 3.8% paraformaldehyde-PBS, and permeabilized by incubation for 15 min with 0.1% Triton-PBS. The cells were blocked with 1% bovine serum albumin-phosphate buffered saline (BSA-PBS), incubated with anti-c-Src or anticortactin antibody for 2 h, washed six times with 0.1% Triton-PBS, and finally incubated with rhodamine-conjugated antimouse immunoglobulin G (IgG) antibody. The cells were extensively washed with PBS and visualized using a fluorescence microscope (Carl Zeiss, Hallbergmoos, Germany).

Results

To understand the role of cortactin in osteoclasts, we first examined the cellular localization of cortactin. Immunocytochemical analyses demonstrated that cortactin was well localized in the actin rings of osteoclasts (Fig. 1A, B, C). In addition, cortactin showed a similar expression pattern to c-Src in osteoclasts (Fig. 1D, E, F). These data suggest that cortactin plays a role in actin ring formation in cooperation with c-Src. To examine the relationship between c-Src and cortactin, we next performed coimmunoprecipitation experiments using an osteoclastic precursor cell line RAW 264.7. Overexpression of cortactin induced tyrosine phosphorylation of cortactin and its association with c-Src in RAW 264.7 cells (Fig. 2). Importantly, overexpression of Csk, which suppresses c-Src function [10], markedly inhibited the association of cortactin with c-Src and the tyrosine phosphorylation of cortactin (Fig. 2). These data support the notion that cortactin functions as a downstream signaling molecule of c-Src.

To evaluate the functional role of cortactin in osteoclasts, we next examined the effect of cortactin on RAW 264.7 cells, which rarely form actin rings, even in the presence of sRANKL [9] (Fig. 3). Overexpression of c-Src clearly stimulated actin ring formation in RAW 264.7 cells (Fig. 3). Furthermore, overexpression of cortactin elicited formation of actin rings (Fig. 3), although cortactin-overexpressing RAW 264.7 cells exhibited little bone resorbing activity. These data indicate that cortactin is implicated in regulation of actin ring formation.

To further analyze the distinctive role of cortactin in osteoclasts, we generated a mutant of cortactin that lacks the actin binding domain (Fig. 4A), and overexpressed the mutant in osteoclasts using an adenovirus system [11]. As shown in Fig. 4B, overexpression of the mutant cortactin disrupted actin ring formation in osteoclasts. More importantly, osteoclastic bone resorption was strongly inhibited by the mutant cortactin (Fig. 4C). Together, the results indicate that cortactin plays a critical role in osteoclastic bone resorption by regulating actin ring formation.

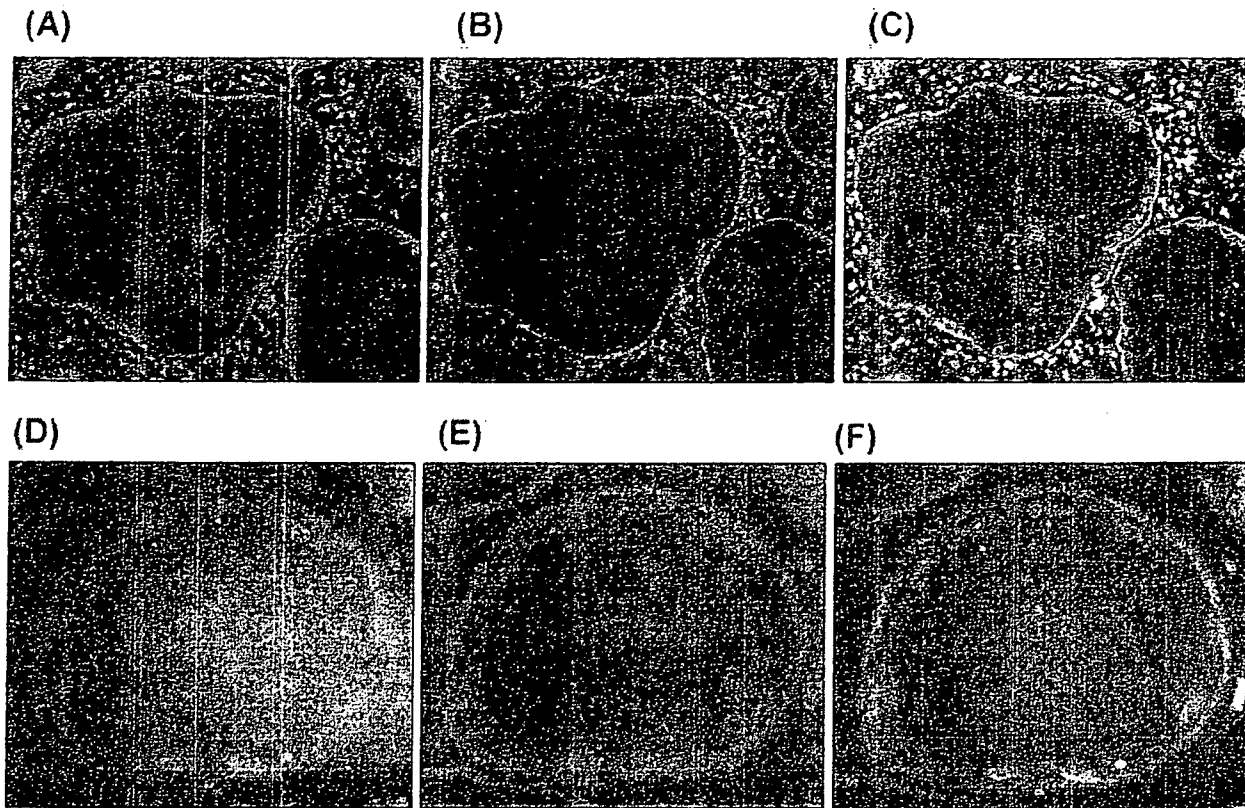


Fig. 1. Localization of cortactin in osteoclasts. Osteoclasts formed from mouse spleen cells were stained with anticortactin antibody (A and D), fluorescein isothiocyanate (FITC)-labeled phalloidin (B), and anti-c-Src antibody E. C and F are merged photographs of A and B, and D and E, respectively. $\times 1000$

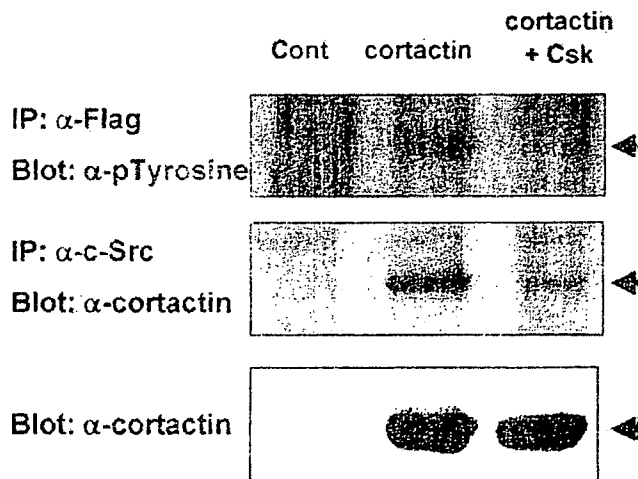


Fig. 2. Tyrosine-phosphorylation of cortactin and its association with c-Src. The lysates of RAW 264.7 cells infected with control adenovirus, or Flag-tagged cortactin with or without Csk adenoviruses, were immunoprecipitated with anti-Flag or c-Src antibody and immunoblotted with antiphosphotyrosine or anticortactin antibody, respectively. The expression of cortactin in the lysates was examined with anticortactin antibody (lower panel). *IP*, immunoprecipitation

Discussion

Several lines of evidence indicate that c-Src is an essential tyrosine kinase for osteoclastic bone resorption [2-4,12]. In this study, we showed that cortactin is expressed specifically in actin rings and is well colocalized with c-Src in osteoclasts. We also confirmed that cortactin functions as a c-Src substrate based on results of the binding of cortactin with c-Src and c-Src-dependent tyrosine phosphorylation. Furthermore, we indicated that overexpression of cortactin elicited formation of actin rings in RAW 264.7 cells that were differentiated into TRAP-positive osteoclasts by sRANKL. Finally, we found that a mutant of cortactin diminished both actin ring formation and bone resorption. Collectively, our data suggest the indispensable role of cortactin in osteoclast function.

Hurst et al. reported that the actin-related protein2/3 (Arp2/3) complex is essential for actin ring formation in osteoclasts [8]. Cortactin has been shown to control actin polymerization through Arp2/3 [13]. Considering that c-Src interacts with and controls cortactin [6], it is most likely that cortactin links c-Src signaling to Arp2/3 in osteoclasts, and thereby regulates actin polymerization. To support this proposed mechanism, we found that Csk, which is an inhibitory kinase for c-Src, inhibited tyrosine phosphorylation of cortactin, its association with c-Src and osteoclastic bone

Fig. 3. Stimulation of actin ring formation of RAW 264.7 cells by cortactin. RAW 264.7 cells were cultured in the presence of soluble receptor activator of NF-kappaB ligand (sRANKL) (10 ng/ml) for 2 days, and infected with control, c-Src, or Flag-tagged cortactin adenovirus. Three days after infection, the cells were determined by tartrate-resistant acid phosphate (TRAP) staining and rhodamine-phalloidin. The number of TRAP-positive multinucleated cells and the number of TRAP-positive multinucleated cells that form actin rings are shown. The photographs show representative cells

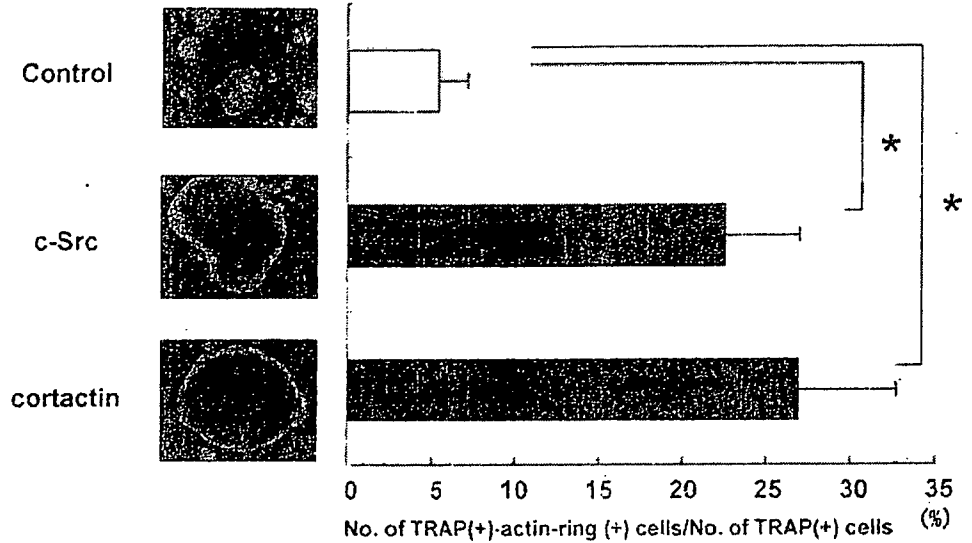
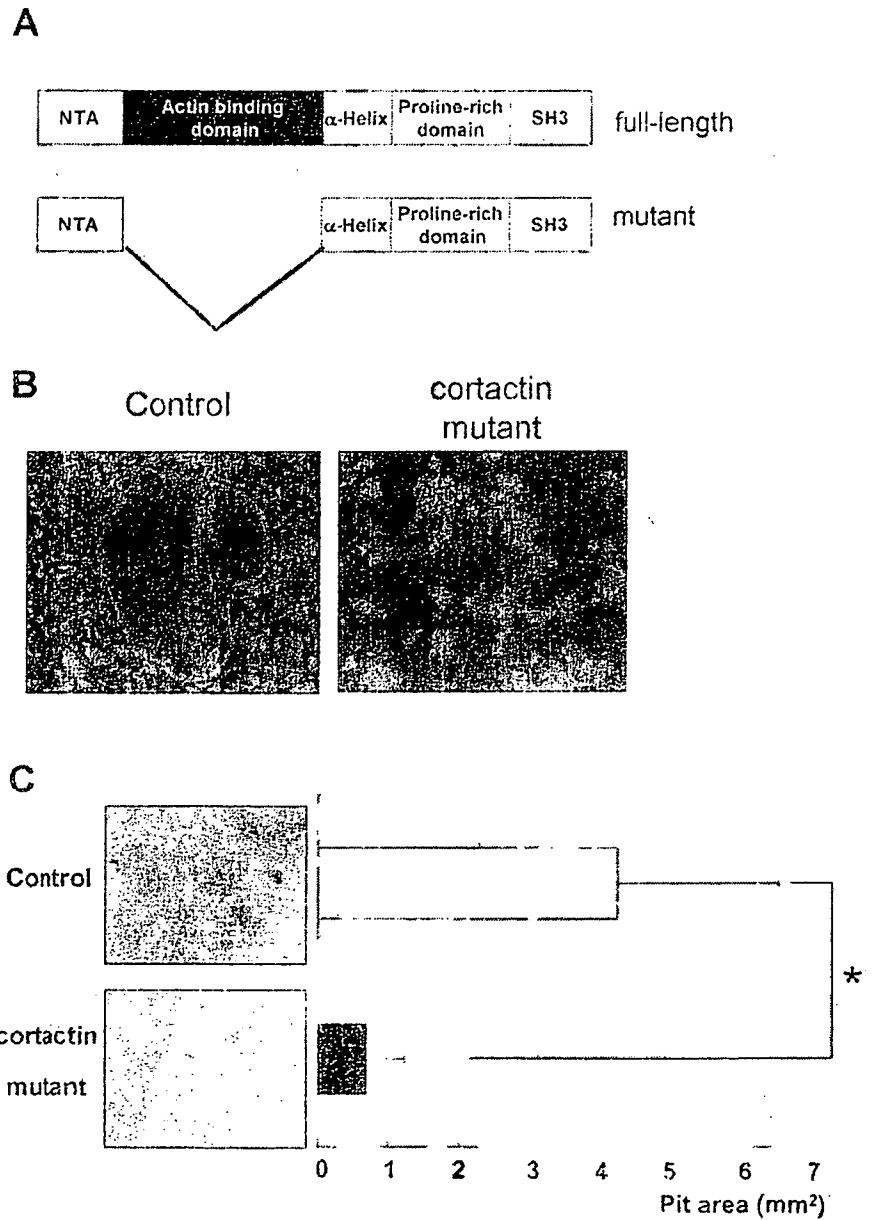


Fig. 4. Disruption of actin ring formation and bone resorption by a mutant cortactin. **A** Schematic diagram of a mutant cortactin. **B** Osteoclasts formed from mouse spleen cells were infected with control or mutant cortactin adenovirus, and 36 h after infection, the cells were stained with rhodamine-labeled phalloidin. **C** Mouse spleen cells were incubated with sRANKL (100 ng/ml) and macrophage colony-stimulating factor (M-CSF) (30 ng/ml) for 4 days and infected with control or mutant cortactin adenovirus; 2 days after infection, the pits were examined



resorption (data not shown). Consistent with our results with the osteoclasts, Destaing et al. showed that cortactin is localized at podosomes of RAW 264.7-cell-derived osteoclasts [14]. However, they also clearly demonstrated that the turnover of cortactin is a few times slower than actin turnover [14]. Thus, it is likely that other components of the actin core are implicated in actin turnover in osteoclasts.

In conclusion, we have provided evidence that cortactin is an important signaling molecule that regulates actin ring formation and bone resorption in osteoclasts. We believe that our findings contribute to understanding the molecular mechanism of bone destruction by osteoclasts.

Acknowledgments We thank Drs. Harold E. Varmus and Thomas Parsons for providing c-Src and cortactin cDNA, respectively. This work was supported in part by the Ministry of Education, Science, Sports and Culture's Grant-in-Aid for Scientific Research A 11307041 (TY), B 15390560 (RN), and C 10671739 (RN), Grant-in-Aid for Scientific Research on Priority Areas B 12137205 (TY), and The 21st Century COE Program (TY, RN).

References

1. Frame MC, Fincham VJ, Carragher NO, Wyke JA (2002) v-Src's hold over actin and cell adhesions. *Nat Rev Mol Cell Biol* 3:233–245
2. Soriano P, Montgomery C, Geske R, Bradley A (1991) Targeted disruption of the c-src proto-oncogene leads to osteopetrosis in mice. *Cell* 64:693–702
3. Boyce BF, Yoneda T, Lowe C, Soriano P, Mundy GR (1992) Requirement of pp60c-src expression for osteoclasts to form ruffled borders and resorb bone in mice. *J Clin Invest* 90:1622–1627
4. Lowe C, Yoneda T, Boyce BF, Chen H, Mundy GR, Soriano P (1993) Osteopetrosis in Src-deficient mice is due to an autonomous defect of osteoclasts. *Proc Natl Acad Sci USA* 90:4485–4489
5. Miyazaki T, Neff L, Tanaka S, Horne WC, Baron R (2003) Regulation of cytochrome c oxidase activity by c-Src in osteoclasts. *J Cell Biol* 160:709–718
6. Wu H, Parsons JT (1993) Cortactin, an 80/85-kilodalton pp60src substrate, is a filamentous actin-binding protein enriched in the cell cortex. *J Cell Biol* 120:1417–1426
7. Li Y, Uruno T, Haudenschield C, Dudek SM, Garcia JG, Zhan X (2004) Interaction of cortactin and Arp2/3 complex is required for sphingosine-1-phosphate-induced endothelial cell remodeling. *Exp Cell Res* 298:107–121
8. Hurst IR, Zuo J, Jiang J, Holliday LS (2004) Actin-related protein 2/3 complex is required for actin ring formation. *J Bone Miner Res* 19:499–506
9. Ikeda F, Nishimura R, Matsubara T, Tanaka S, Inoue J, Reddy SV, Hata K, Yamashita K, Hiraga T, Watanabe T, Kukita T, Yoshioka K, Rao A, Yoneda T (2004) Critical roles of c-Jun signaling in regulation of NFAT family and RANKL-regulated osteoclast differentiation. *J Clin Invest* 114:475–484
10. Takayanagi H, Juji T, Miyazaki T, Iizuka H, Takahashi T, Isshiki M, Okada M, Tanaka Y, Koshihara Y, Oda H, Kurokawa T, Nakamura K, Tanaka S (1999) Suppression of arthritic bone destruction by adenovirus-mediated csk gene transfer to synoviocytes and osteoclasts. *J Clin Invest* 104:137–146
11. Hata K, Nishimura R, Ueda M, Ikeda F, Matsubara T, Ichida F, Hisada K, Nokubi T, Yamaguchi A, Yoneda T (2005) A CCAAT/enhancer binding protein beta isoform, liver-enriched inhibitory protein, regulates commitment of osteoblasts and adipocytes. *Mol Cell Biol* 25:1971–1979
12. Horne WC, Sanjay A, Bruzzaniti A, Baron R (2005) The role(s) of Src kinase and Cbl proteins in the regulation of osteoclast differentiation and function. *Immunol Rev* 208:106–125
13. Zhu J, Zhou K, Hao JJ, Liu J, Smith N, Zhan X (2005) Regulation of cortactin/dynamain interaction by actin polymerization during the fission of clathrin-coated pits. *J Cell Sci* 118:807–817
14. Destaing O, Saltel F, Geminard JC, Jurdic P, Bard F (2003) Podosomes display actin turnover and dynamic self-organization in osteoclasts expressing actin-green fluorescent protein. *Mol Biol Cell* 14:407–416

REVIEW ARTICLE

Takanobu Nakase · Hideki Yoshikawa

Potential roles of bone morphogenetic proteins (BMPs) in skeletal repair and regeneration

Received: July 5, 2006 / Accepted: July 20, 2006

Key words bone morphogenetic protein · skeletal repair · regeneration · gene expression · orthopedics

Introduction

Bone morphogenetic protein (BMP) was originally discovered by Urist in 1965 as a bone-inducing substance in an ectopic site [1], and the term “BMP” was first described by Urist and Strates in 1971 [2]. By 1988, molecular clones, as well as the amino-acid sequences of BMP had been characterized from a highly purified preparation obtained from bovine bone [3]. In 1993, murine molecular clones from murine osteosarcoma had also been identified, and they became available for animal experimental systems [4,5] and enabled the performance of various investigations based on molecular technologies. To date, at least 20 members of the BMP family have been identified. In addition to its bone-inducing activity, BMP is now thought to have essential and multifunctional roles in various other organs during morphogenesis. Now, “BMP” should be better recognized as “body morphogenetic protein” [6].

From the viewpoint of clinical applications in orthopedic medicine, several members of the BMP family are attracting considerable attention as promising therapeutic tools for skeletal regeneration and as target molecules for the treatment of skeletal disorders. Previous investigations showed that BMP-2, -4, and -7 stimulated osteogenic and chondrogenic differentiation via BMP receptor (BMPR)

types I and II [7–9]. Smad mediates the intracellular signaling of these BMPs [10]. Another BMP, cartilage-derived morphogenetic protein (CDMP)-1 also known as growth and differentiation factor-5 (GDF-5), reportedly shows unique activities, such as the promotion of chondrogenic differentiation and the induction of tendon tissue in vivo [11,12]. Recombinant BMP-2 and -7 proteins have already been in clinical use in the United States and Europe for problematic trauma cases such as open fractures and nonunions [13,14]. The clinical outcomes have been reported as encouraging.

This article reviews the current findings regarding BMP signaling underlying the process of skeletal repair and regeneration. Which BMPs are involved, and in what manner are they involved in the process of bone repair and regeneration? How are BMPs induced in various orthopedic conditions? In some instances, the BMPs play physiological roles, while in other instances, they play pathological roles. The findings will provide a key to understanding the physiological and pathological natures of BMPs and BMP signals in various orthopedic conditions, leading to novel therapeutic formulations aimed at less invasive and more promising treatment of orthopedic injuries and disorders.

Skeletal repair

Fracture repair

Fracture repair involves a number of regenerative events initiated by the breakage of bone tissue. Cells at fracture sites, i.e., periosteum, para-fracture soft tissue, intramedullary canal, and bone cortex, respond to the impact of the fracture. They proliferate and differentiate into cells of osteogenic and chondrogenic lineages, and this is followed by membranous and endochondral ossification, forming a “fracture callus”, leading to fracture union [15] (Figs. 1 and 2).

The sequential process of fracture repair is a repetition of embryonic bone development. However, distinct from

T. Nakase (✉)
Department of Orthopaedic Surgery, Hoshigaokakoseinenkin
Hospital, 4-8-1 Hoshioka, Hirakata, Osaka 573-8511, Japan
Tel. +81-72-840-2641; Fax +81-72-840-2266
e-mail: tnakase@ff.ij4u.or.jp

H. Yoshikawa
Department of Orthopaedic Surgery, Osaka University Graduate
School of Medicine, Suita, Japan

T. Nakase is a recipient of the JSBMR Academic Award 2005.

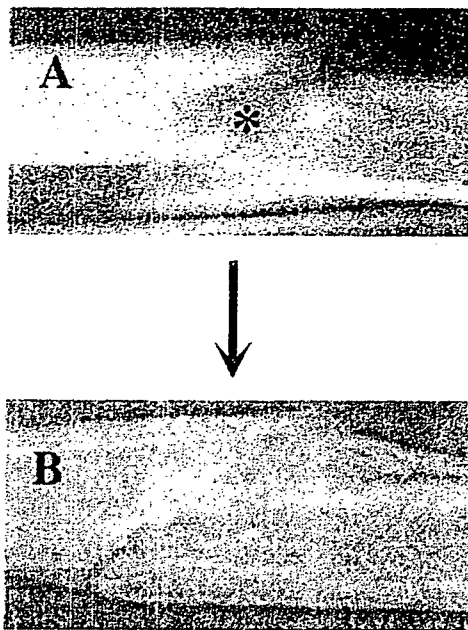


Fig. 1. Radiographic findings, showing repair of human fractured bone. **A** Asterisk indicates radiolucent line, showing a fracture. **B** Fractured bones are united by fracture callus

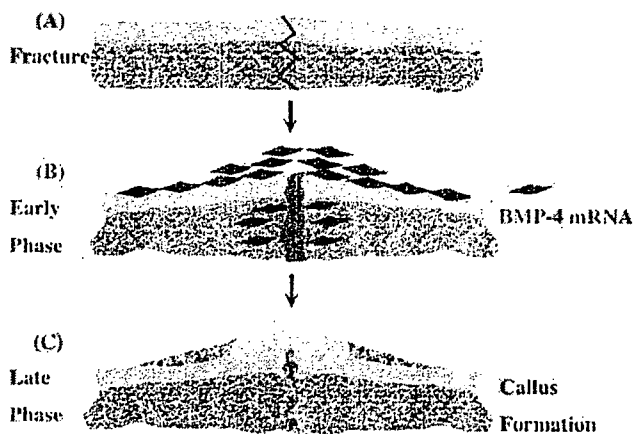


Fig. 2. Localization of bone morphogenetic protein-4 (*BMP-4*) mRNA during the process of fracture repair. **A** Fracture at the mid-shaft of the long bone. **B** Early phase: formation of hematoma at the fracture site, as well as proliferation of immature callus-forming cells in the periosteum, para-fracture soft tissue, and intramedullary cavity. *BMP-4* mRNA is induced in the early phase in these immature cells. **C** Late phase: *BMP-4* mRNA is no longer detected during the late phase. However, prominent fracture calluses have formed in the periosteal and intramedullary regions

embryogenesis, some kind of stimulus is a prerequisite for the induction of the fracture repair process [15,16]. Our previous in situ hybridization study showed that *BMP-4* mRNA was induced in the early phase of fracture repair in the less-differentiated cells at callus-forming sites, such as periosteum, marrow cavity, and surrounding soft tissue. In the later stages, *BMP-4* mRNA could no longer be detected (Fig. 2) [15]. These findings have been confirmed by semi-quantitative reverse transcription-polymerase chain

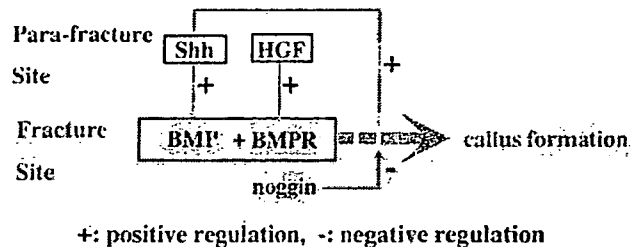


Fig. 3. Hypothetical scheme showing a "BMP network" in the mechanism of fracture repair. BMP and BMP receptor (*BMPR*) induced at the fracture site initiate callus formation. Sonic hedgehog (*Shh*) and hepatocyte growth factor (*HGF*) synthesized at the para-fracture site positively regulate BMP-dependent callus formation, whereas noggin inhibits the effect of BMP on callus formation

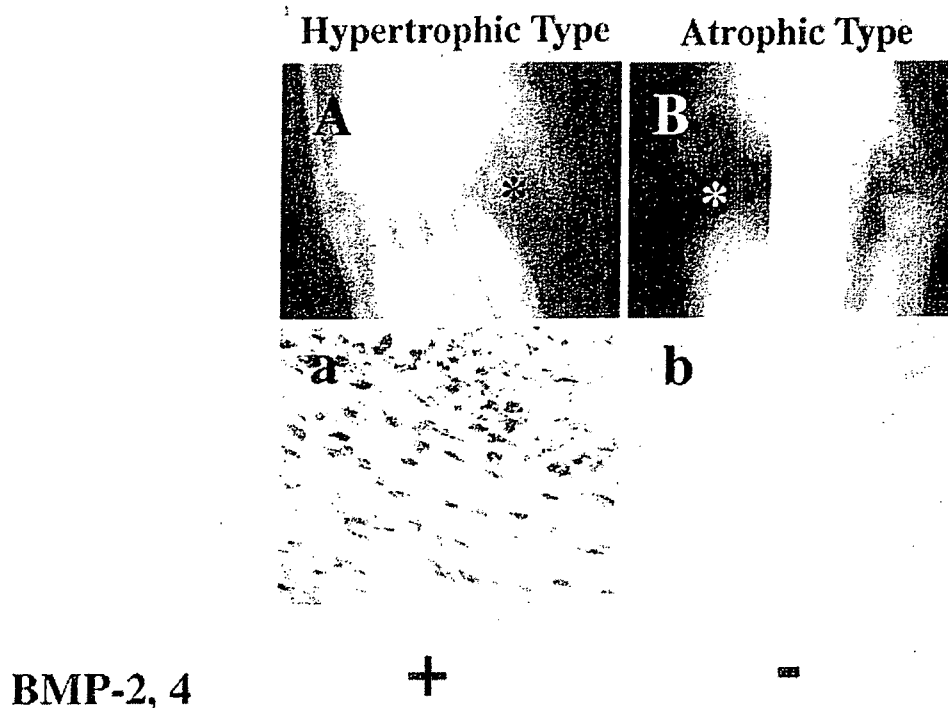
reaction (RT-PCR) [15]. Similar findings have been reported in several other studies. On immunohistochemical analysis, using specific antibodies for *BMP-2*, *-4*, and osteogenic protein (*OP*)-1 (*BMP-7*), these members of the BMP family were shown to be upregulated in the early phase of fracture-healing in immature cells, and continuous expression was observed throughout the healing process [17,18]. In other reports using a rat fracture model, these members of the BMP family were upregulated in the early phase, but such induction was decreased and delayed in older rats [19].

BMP signaling molecules, such as *BMPR* types IA, IB, and II have also been identified in locations similar to those for BMPs during fracture healing [17,20]. The BMPs and BMP signaling components are localized at callus-forming sites, suggesting the key roles of BMPs in fracture repair, and raising the possibility of their use as target or therapeutic molecules for fracture treatment. For example, *BMP-4* gene transfer into the periosteum in the early phase dramatically enhanced fracture healing in a rat model [21].

In addition to BMP itself, other BMP-related factors have been identified during fracture healing. Sonic hedgehog (*Shh*), a stimulator of BMP-dependent chondrogenic and osteoblastic differentiation [22,23], has been identified at the para-fracture site in the early phase, and may promote BMP-induced callus formation [24]. Hepatocyte growth factor (*HGF*) is located at the para-fracture site, with its receptor *c-Met* [25]. In vitro studies have shown that *HGF* upregulates *BMPR* expression in mesenchymal cells, and may contribute to BMP-dependent callus formation [25]. In addition to these positive regulators of BMP signaling, *noggin* is reportedly co-localized with *BMP-4* throughout the healing process [26]. Overexpression of *noggin* reportedly inhibits BMP-dependent chondrogenesis [26], and *noggin* may negatively regulate BMP-induced callus formation during fracture repair. These current findings suggest that the process of fracture repair is regulated by various BMP-related factors located in distinct areas, forming a "BMP network" (Fig. 3).

Although most investigations have been performed using animal models, several current studies have shown the actual expression of BMPs in human situations. *BMP-2*, *-4*, and *-7*, as well as *BMPR* types IA, IB, II, and *Smad 1*, have

Fig. 4. Expression and localization of BMP-2 and -4 mRNA in surgical specimens of hypertrophic (A and a) and atrophic (B and b) callus. A and B: Radiographic findings; a and b: in situ hybridization, using BMP-2-specific probes. BMP-2 (a and b) and BMP-4 (data not shown) mRNAs are localized in immature fibroblastic cells in hypertrophic callus (a; asterisk area in A), but not in atrophic callus (b; asterisk area in B). These findings were confirmed by reverse transcription-polymerase chain reaction (RT-PCR)



been detected in human fracture callus specimens [28,29]. However, the ubiquitous expression of these BMP family members did not suggest specific roles of the BMP family members in fracture healing in human situations. In our current unpublished observations, BMP-2 and BMP-4 mRNA and proteins were identified in tissue from hypertrophic (viable) nonunion callus, but they were not identified in tissue from atrophic (nonviable) nonunion callus (Fig. 4); these findings suggest possible roles of BMPs in callus formation in human situations.

To summarize, BMPs seem to play crucial roles in the events of fracture healing. Several BMP family members, such as BMP-2, -4, and -7, will certainly serve as therapeutic molecules in fracture treatment. The mechanisms of BMP induction in the early phase of fracture repair might provide a key to solving the mechanism of bone regeneration. The series of current findings regarding the roles of BMP and related factors in fracture repair will provide a key for the formulation of therapeutic strategies for less invasive and more definitive fracture treatment.

Tendon repair

BMPs are not only involved in bone repair but also in tendon repair. The BMPs involved in tendon repair are GDF-5 (CDMP-1/BMP-14), GDF-6 (CDMP-2/BMP-13), and GDF-7 (CDMP-3/BMP-12). These molecules induce tendon formation at ectopic sites in rats [12].

CDMP-1 has been identified in tendon tissue undergoing repair in the shoulder joint (rotator cuff) in human specimens [30]. Upregulated localization of CDMP-1 at the torn site has been observed. Both CDMP-1 mRNA and the protein were predominantly localized in cells at the torn edge

and bursa side (Fig. 5). Various animal studies using gene knockout mice have revealed the potential roles of these molecules in tendon repair [31,32] and they are becoming promising therapeutic agents for tendon surgery [33].

Mechanical stress and skeletal regeneration

Induction of the *BMP* gene is a particularly important focus of interest in orthopedic medicine, because it holds a key to solving the central mechanism of skeletal regeneration. Mechanical stress is one of the crucial factors stimulating skeletal regeneration, and our current findings suggest that mechanical stress may induce BMP expression.

Distraction osteogenesis

The effect of mechanical stretching on skeletal regeneration has been dramatically corroborated by such surgical procedures as distraction osteogenesis, a principle first introduced by Ilizarov [34]. Gradual distraction between the bone fragments after osteotomy induces bone regeneration within the distraction gap (Fig. 6). This regenerative effect has been characterized by the gene expression of *BMP-2* and *BMP-4* in the lengthened callus [35]. *BMP-2* and -4 mRNAs were upregulated just after the osteotomy, as they are in fracture repair. However, after the beginning of the distraction, the gene expressions of *BMP-2* and *BMP-4* were shown to have increased up to tenfold by upregulation. In contrast, the level of GDF-5 and BMP-6 mRNA did not seem to be affected by the distraction stress (Fig. 7) [35]. These findings indicate the positive effect of

Fig. 5. A Localization of cartilage-derived morphogenetic protein-1 (*CDMP-1*) mRNA and protein in torn rotator cuff. *CDMP-1* is predominantly localized in cells at the torn edge and bursa side. *TS*, Torn edge side; *BS*, bursa side; *JS*, joint side; *OS*, opposite side to torn edge. **B** Cell count analysis revealed a marked increase in *CDMP-1*-positive cells in the torn edge and bursa side

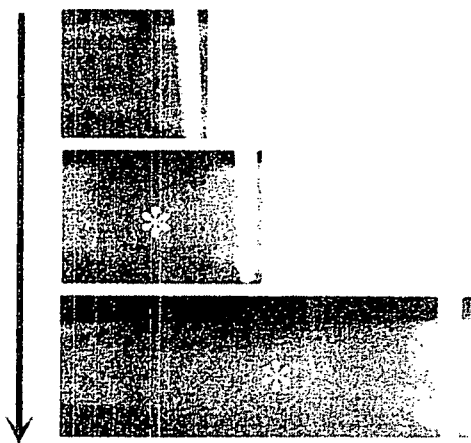
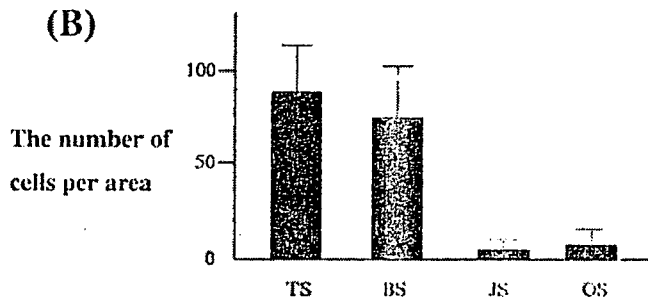
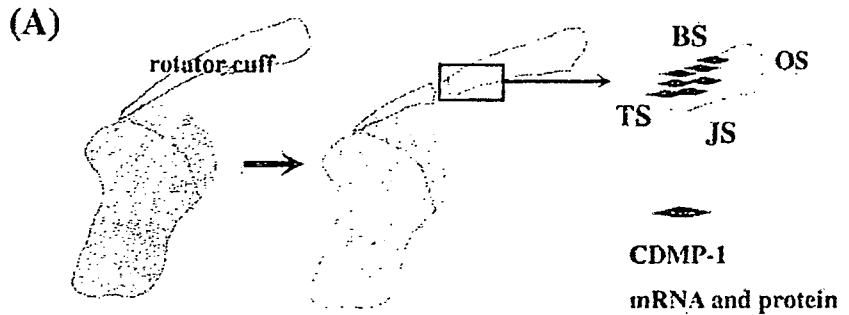


Fig. 6. Radiographic findings showing gradual distraction osteogenesis. Regenerative bone formation is seen in the distraction gap (asterisk)



Fig. 7. Schematic illustration, showing lengthening callus formed in the distraction gap. During the distraction phase, *BMP-2* and *-4* mRNAs are induced, whereas the expression of growth and differentiation factor-5 (*GDF-5*) and *BMP-6* mRNAs is not affected by distraction stress

mechanical tension stress on the induction of gene the expression of *BMP-2* and *BMP-4*.

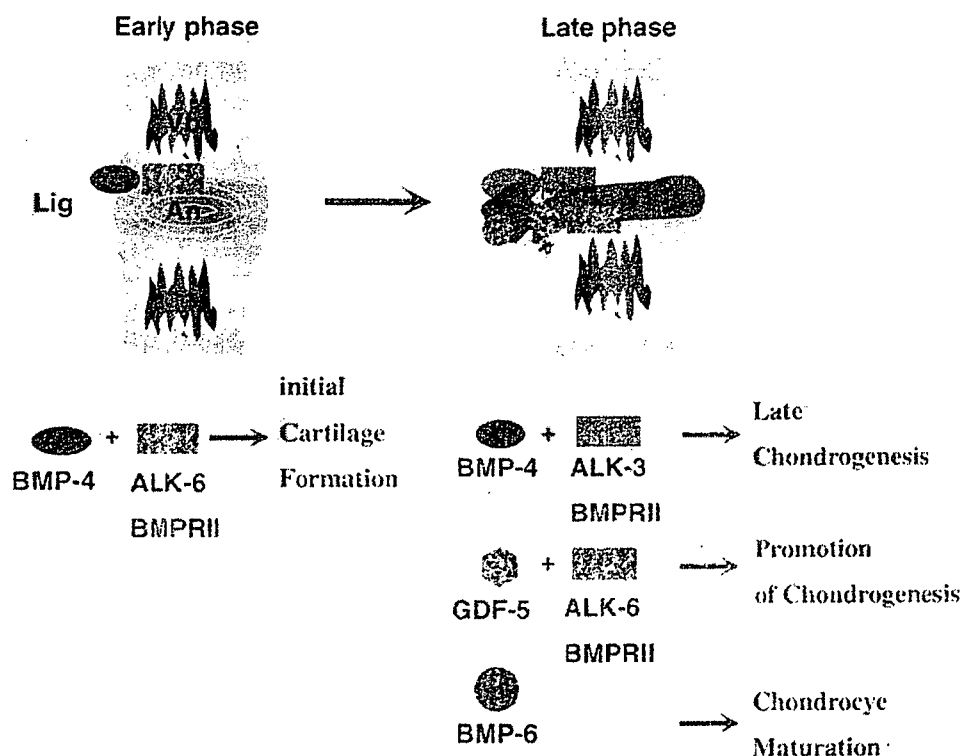
Mechanical overload-induced spondylosis

Mechanical overload sometimes induces bone regeneration. This phenomenon often occurs at the bone-cartilage-tendon junction. One example of this phenomenon occurs at the disco-vertebral junction in some spinal regions [36] (Fig. 8). In a mouse model of spondylosis induced by resection of the posterior components of the cervical spine, prominent and rapid growth of an osseous spur in the anterior portion of the affected spine was seen [37]. Such a phenomenon is similar to that observed in human spondylosis, in which chronological histological observations show a process of bone regeneration resembling endochondral ossification. Molecular mechanisms underlying the sequential process of spondylosis in the mouse model have been investigated by in situ hybridization, using specific cDNAs for BMP-related factors [38]. In the early stage, cells in the anterior margin of the disc beside the attachment of the spinal ligament (annulus-ligament complex; ALC) proliferate, showing metaplasia, into round chondrocyte-like cells. *BMP-4* mRNA is localized predominantly in cells in the anterior margin of the disc (ALC), together with *ALK-6* (*BMPRI* and *II*) mRNA. *GDF-5* and *BMP-6* mRNAs are not detected at this stage. In the late stage, fibroblastic cells are almost totally replaced by mature chondrocytes. Enlargement of cartilaginous tissues, together with osteophyte tissue, is observed in the anterior margin of the disc. Cells positive for *BMP-4* decrease, whereas *GDF-5* and *BMP-6* mRNAs are localized in cells undergoing chondrogenesis.

Fig. 8. **A** Radiographic findings showing osteophyte formation (*arrow*) in human cervical spondylosis. **B** Histological findings showing round chondrocyte-like cells in the anterior margins of the disc-vertebral junction in human spondylosis. Hematoxylin and Eosin Staining, $\times 100$



Fig. 9. Proposed scheme of the involvement of BMP signals underlying spondylosis produced in a mouse model. BMP-4 mRNA is induced at the anterior annulus-ligament complex, and ALK-6 (BMPR IB) and BMPR II mediate BMP-4-dependent initial chondrogenesis. In the late phase, BMP-4 regulates late chondrogenesis via ALK-3 (BMPR IA)/BMPR II, and GDF-5 promotes chondrogenesis via ALK-6/BMPR II. BMP-6 mRNA is activated and BMP-6 possibly stimulates chondrocyte maturation. (*Lig*, ligament; *Vb*, vertebral body; *An*, annulus fibrosus)



ALK-3 (BMPR IA) mRNA begins to appear at this stage, together with the ALK-6 and BMPR II mRNA that is already present [38].

Together with the reported roles of these molecules in endochondral ossification, the molecular mechanisms underlying the above mouse model [38] are thought to be as follows (Fig. 9): BMP-4/ALK-6 is activated, most likely by the mechanical stimuli, and regulates initial chondrogenesis at the ALC. BMP-4/ALK3 and GDF-5/ALK-6 promote cartilage formation and enlargement of the cartilaginous matrix [38]. Such BMP signaling may act as a mediator in the process of mechanical overload-induced bone regeneration.

Pathological skeletal disorders

Skeletal regeneration sometimes leads to pathological conditions in orthopedic medicine. Newly generated osseous tissues cause problematic phenomena, such as neurovascular compression/irritation, joint contractures and pain. Current reports suggest the involvement of BMPs in such conditions and possible roles of BMPs as therapeutic targets in skeletal disorders.

Ossification of the spinal ligament

Ossification of the spinal ligament or ligamentum flavum is a pathologic condition leading to compression of the spinal

cord and nerve roots, sometimes causing severe myeloradiculopathy. The cause of this disease is not known, but recent reports indicate the possibility of an association between the onset of the condition and the genetic background [39]. Previous immunohistochemical studies showed the local expression of BMP and its receptors in surgical specimens of ossification of the ligamentum flavum (OLF) [40] and ossification of the posterior longitudinal ligament [41], and suggest the possible involvement of BMP in the pathogenesis of this ossification.

Many patients with ossification of the spinal ligament have subclinical conditions [42]; symptomatology depends on the degree of the narrowing of the canal caused by the increased ossified mass [43]. Therefore, identifying local candidate factors involved in the progression of the condition is important. We studied the involvement of CDMP-1 in OLF tissues, by immunohistochemistry and in situ hybridization [44]. CDMP-1 was synthesized by fibroblasts and chondrocytes in the ossified regions, whereas it was not detected in nonossifying regions (Fig. 10). CDMP-1 has been reported as factor promoting chondrogenesis [11]; the findings suggest that CDMP-1 may be involved in the progression of ossification. CDMP-1 may become a therapeutic target for the progression of ossification of the spinal ligament.

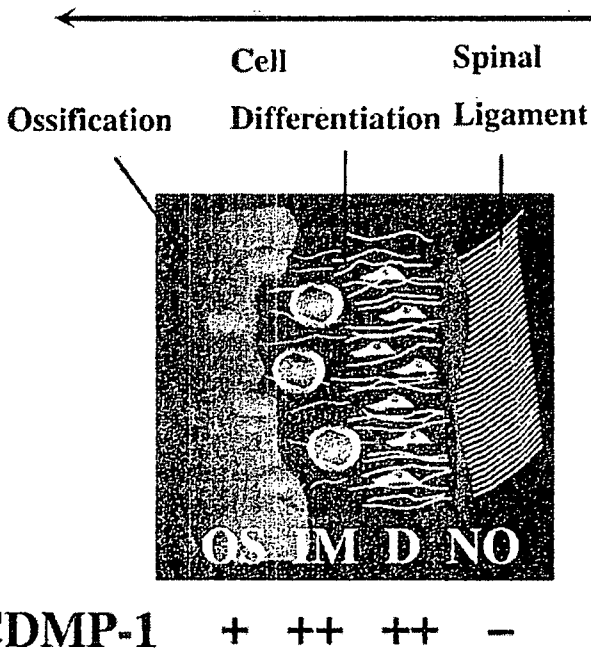


Fig. 10. Proposed model of the localization of CDMP-1 mRNA and protein in the cellular mechanisms of progression of ossification of the ligamentum flavum (OLF). CDMP-1 mRNA and protein are not localized in cells in the nonossifying regions (NO), whereas CDMP-1 is localized in fibroblastic cells in the zone initiating ossification distant from the ossification front (D), in chondrocytes in the intermediate zone (IM), and in cells in the ossification front (OS)

Benign tumorous conditions: osteochondroma and osteoid osteoma

Osteochondroma, also known as an exostosis, is one of the common benign tumorous conditions in skeletal disorders. The condition is characterized by the formation of new osteochondrogenic tissue, called a "cartilage cap" [45] (Fig. 11). The outer growth of a cartilage cap sometimes leads to orthopedic problems such as pain, limitation of range of motion, and compression of neurovascular structures. Our previous studies [46,47] showed that BMP-2 and BMP-4 proteins and mRNAs were identified within mesenchymal cells positive for type III collagen in the outer layer of the cartilage cap, and within chondrogenic cells positive for type II collagen in the inner layer. BMP-2 mRNA, a receptor for BMP-2 and -4, has been identified in the chondrocytes in the inner layer (Fig. 12). These findings suggest the possible action of BMP-2/4-BMP-2 receptor (BMP-2R) pathways in the pathogenesis underlying the growth of osteochondromas, and BMP-2 and -4 could become target molecules for the treatment of osteochondromas.

In addition, the involvement of BMP-2 and -4 in another benign bone tumor has been reported [47,48]. Osteoblastoma is one of the benign tumorous conditions characterized by an osteoid nidus. The nidus is located within the center of the tumor, surrounded by sclerotic bone formed due to an osteoblastic response within the nidus. BMP-2 and -4 have been immunohistochemically identified in cells in the nidus, suggesting the possible involvement of BMP-2 and -4 in the osteoblastic reaction.

Osteoarthritis (OA)

Osteoarthritis (OA) is a common orthopedic disease based on the age-related regeneration of joint cartilage; regenerative changes in the articular cartilage, as well as osteophyte formation, are the essential characteristics of the condition (Fig. 13).

The localization and expression of BMP-2 and -4 have been extensively studied by in situ hybridization and immunohistochemistry [49]. BMP-2 and BMP-4 mRNA and protein were scarcely detected in normal adult articular



Fig. 11A,B. Radiographic findings showing osteochondroma. A X-ray showing osteochondroma expanding on the cortical bone (arrow). B Magnetic resonance imaging (MRI) showing cartilage cap (arrow)